Supplementary Material

Contents:

Supplementary Figures and Schemes

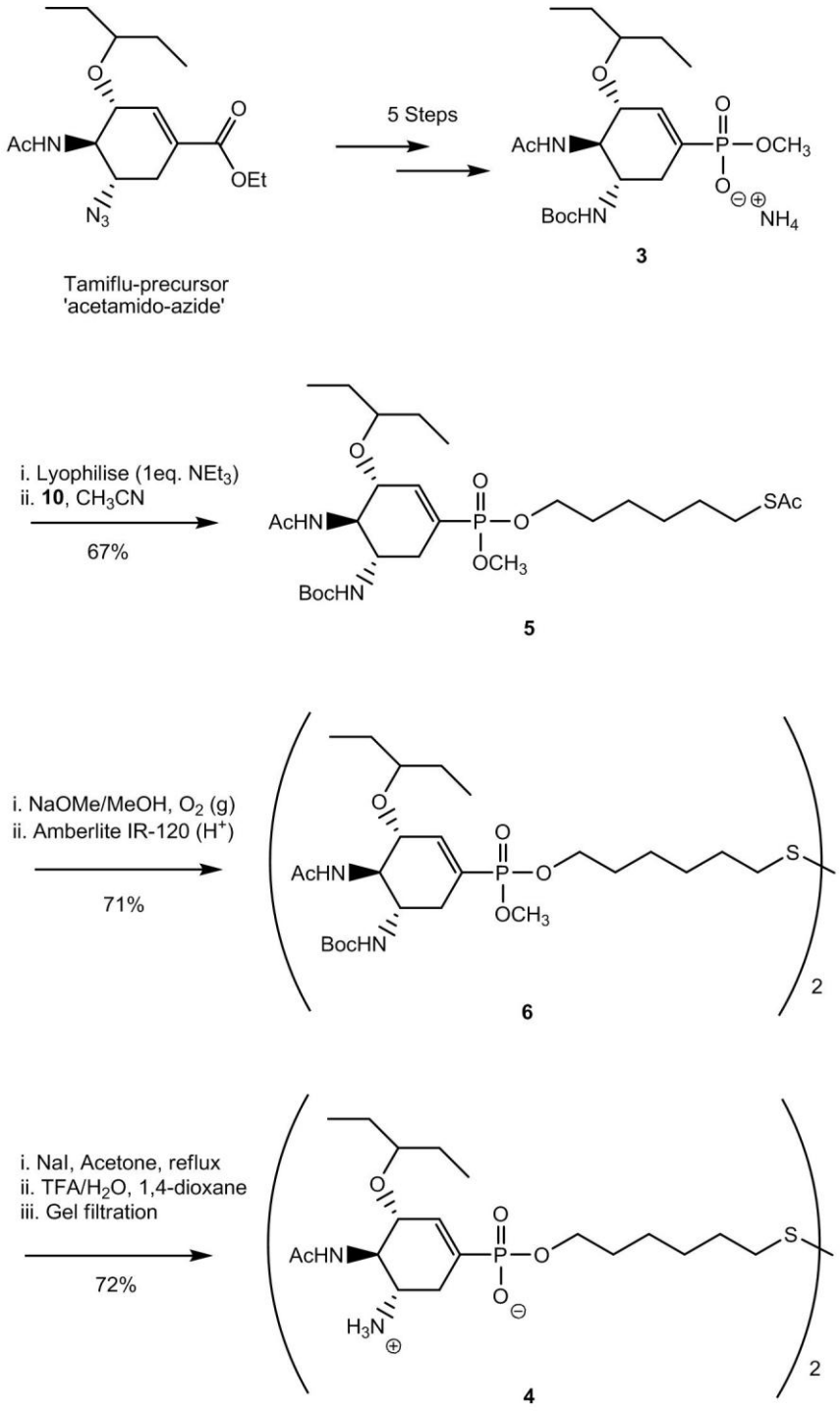

Scheme S1: Synthesis of dimerised phospha-oseltamivir **4** (for ‘small Tamigold’ and ‘large TamiGold’)

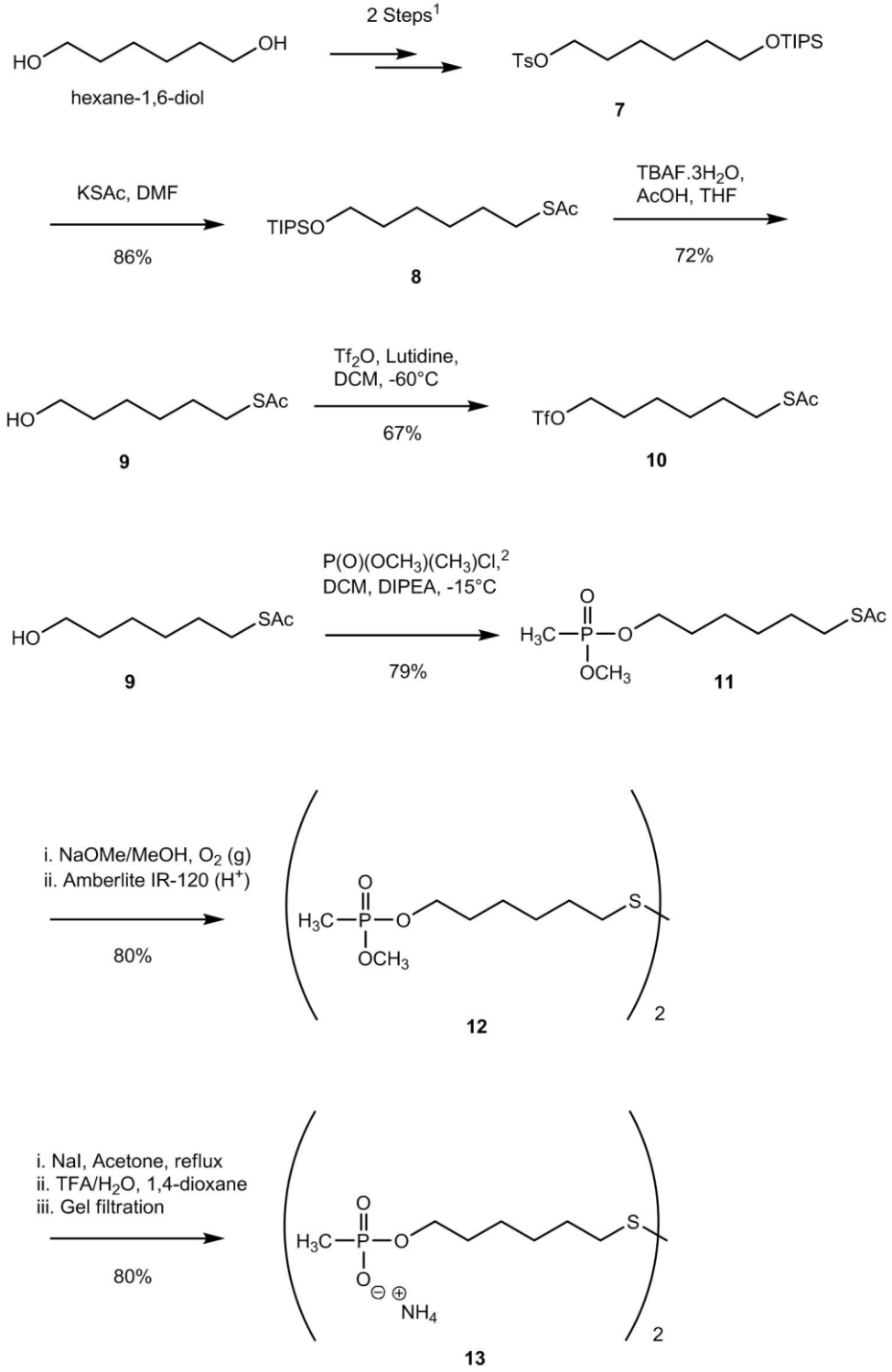

Scheme S2: Synthesis of dimerised spacered methylphosphonate (for ‘small’ control particles)

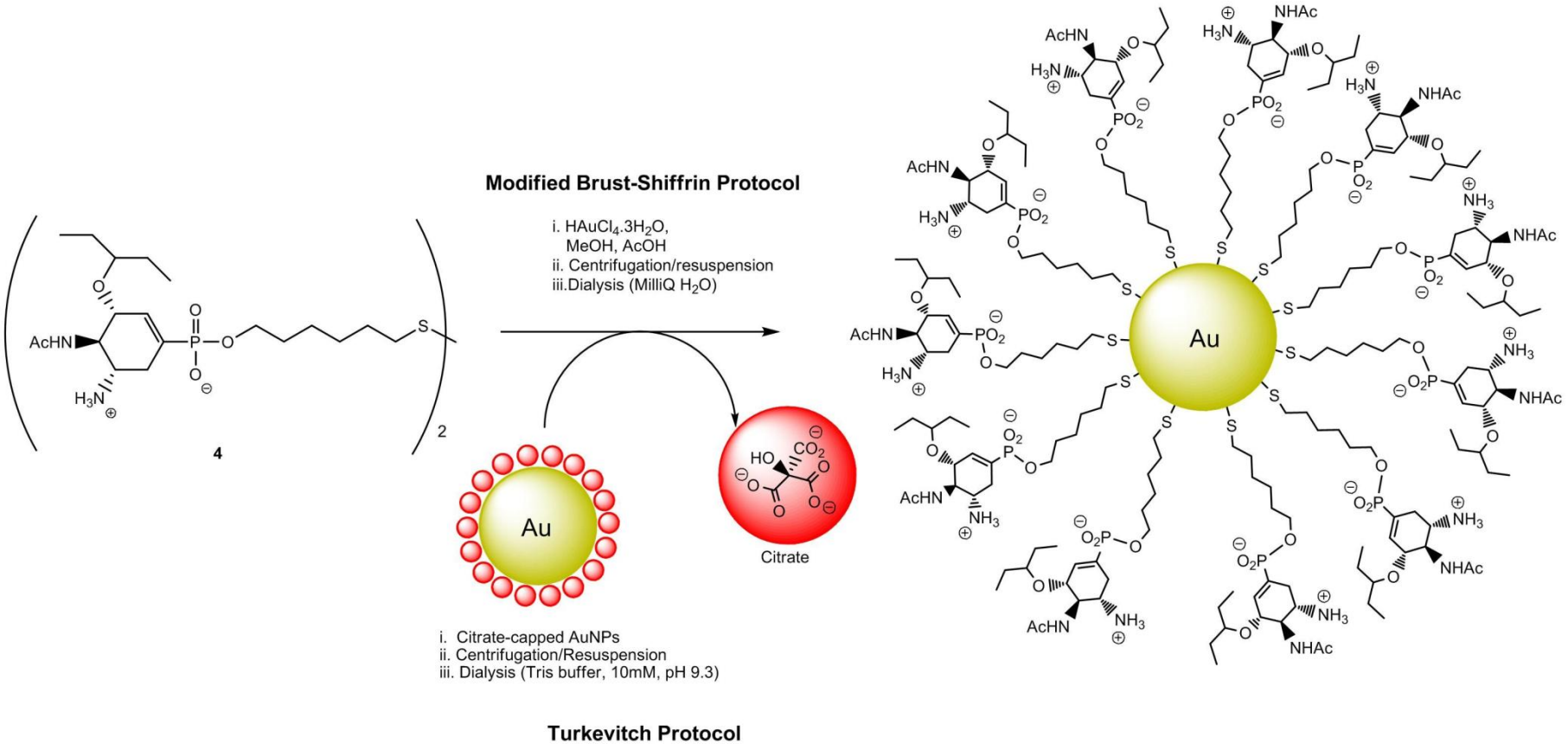

Scheme S3: Synthesis of small and large phospha-oseltamivir-stabilised gold nanoparticles (“small TamiGold” and “large TamiGold”)

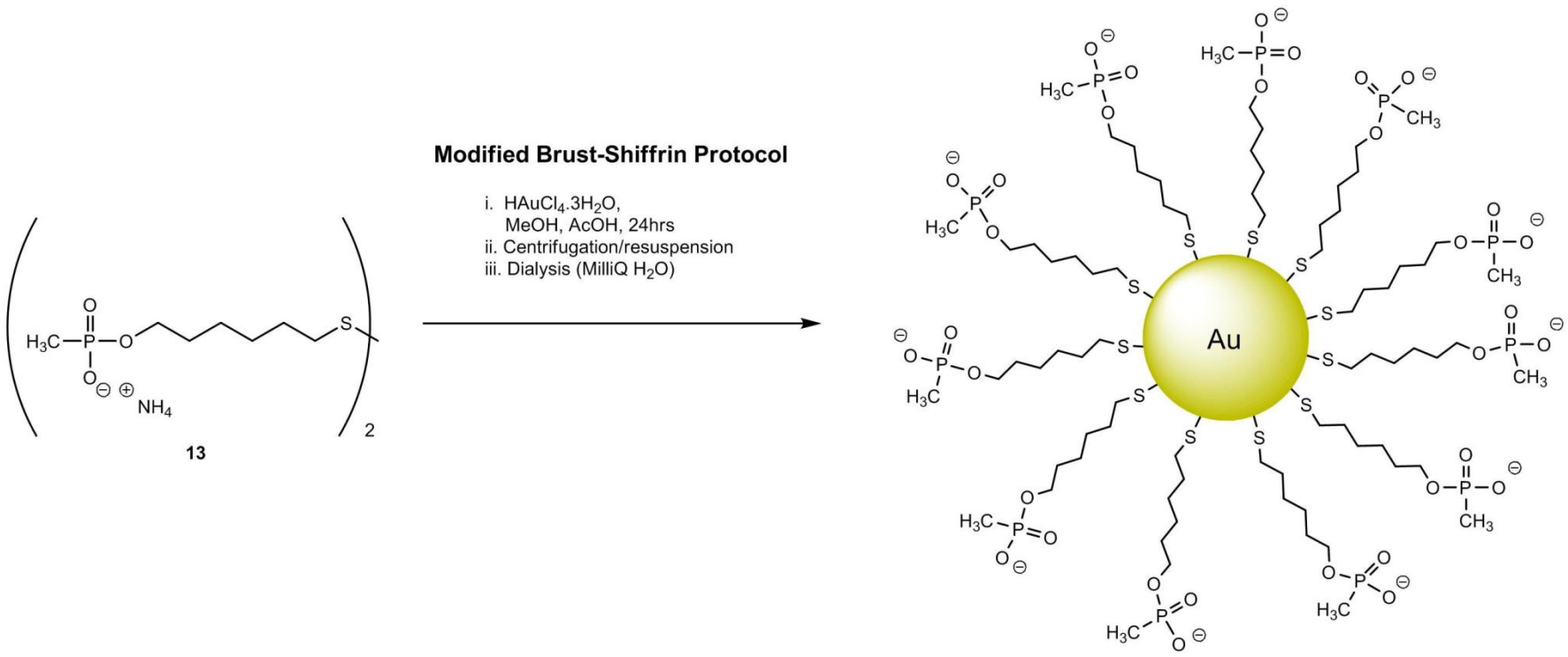

Scheme S4: Synthesis of (small) methylphosphonate-stabilised gold nanoparticles as control for inhibition assays

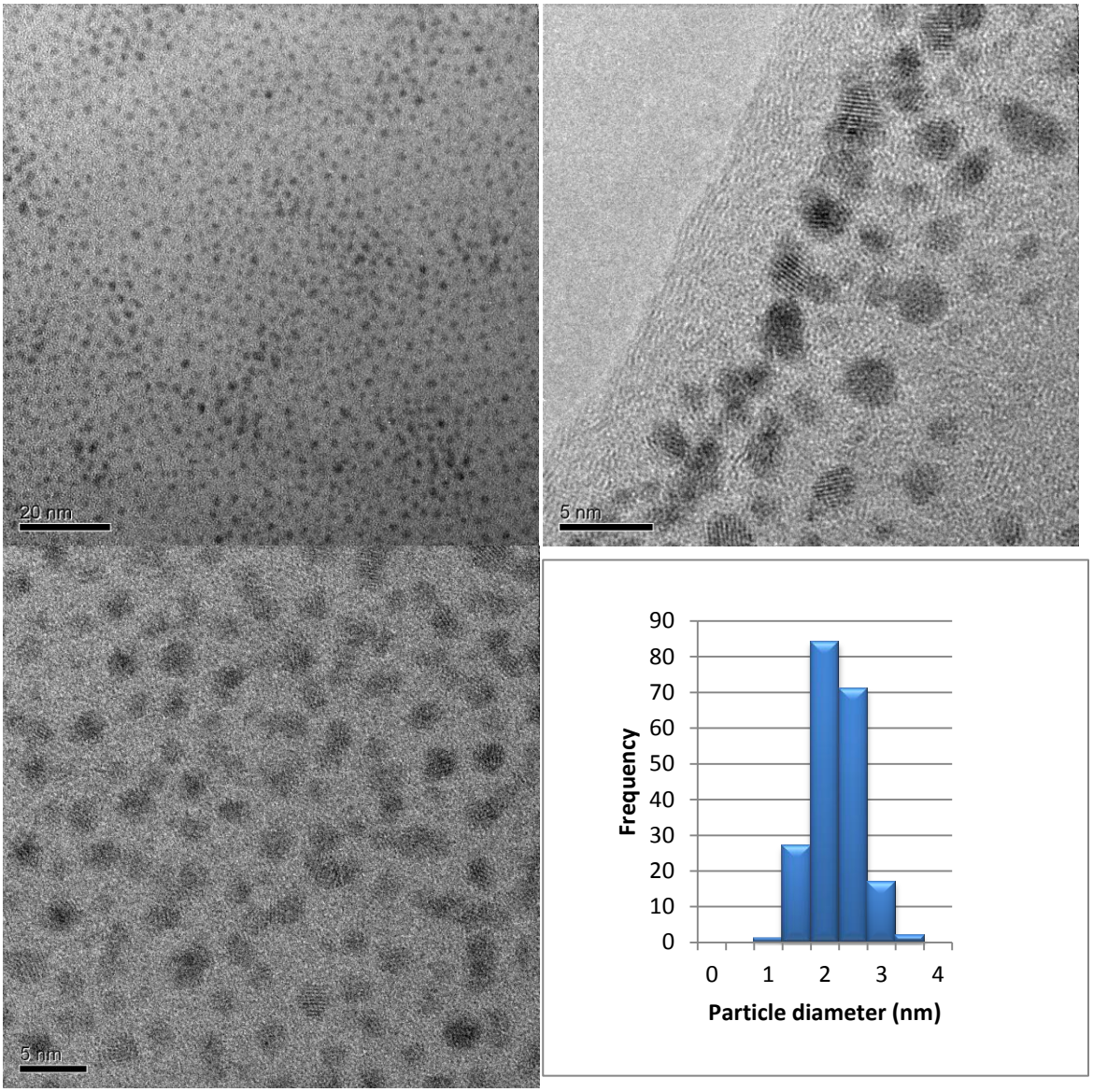

Particle Count	*Mean diameter (nm)*	*sdev (nm)*
202	2.0	0.4

Fig. S1: HR-TEM analysis of small phospha-oseltamivir-stabilised gold nanoparticles ("small TamiGold")

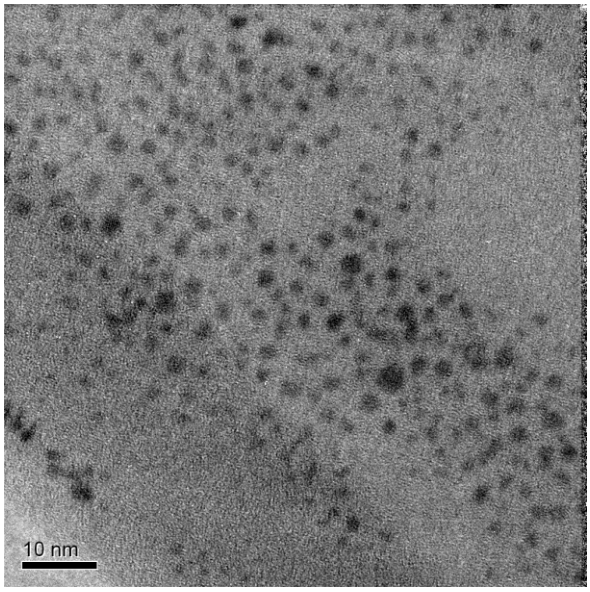

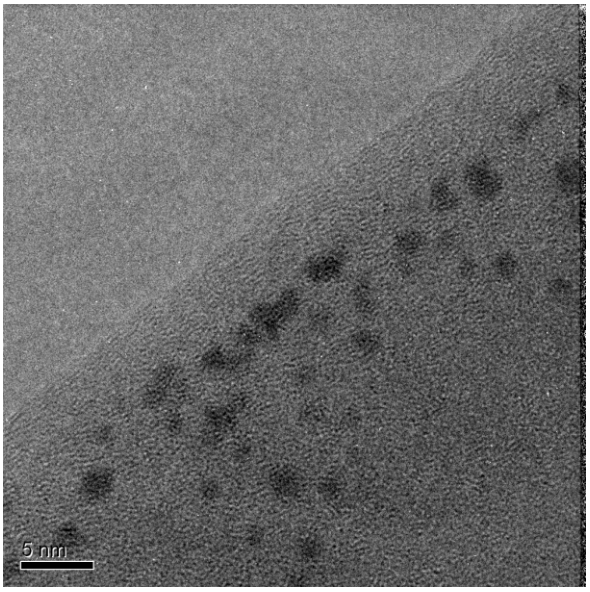

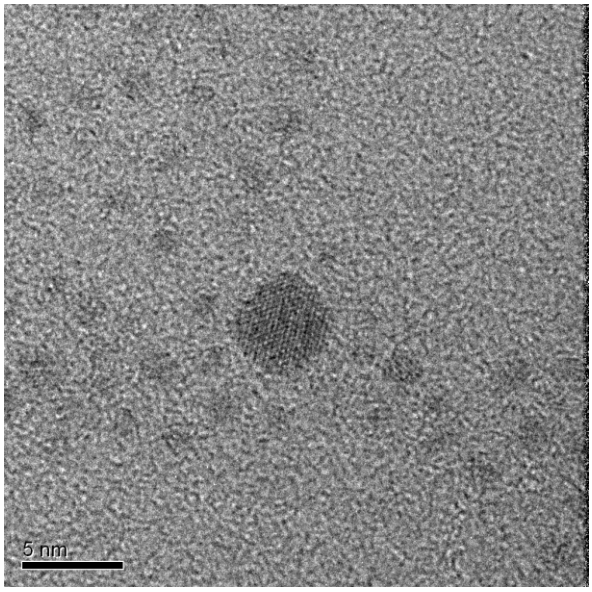

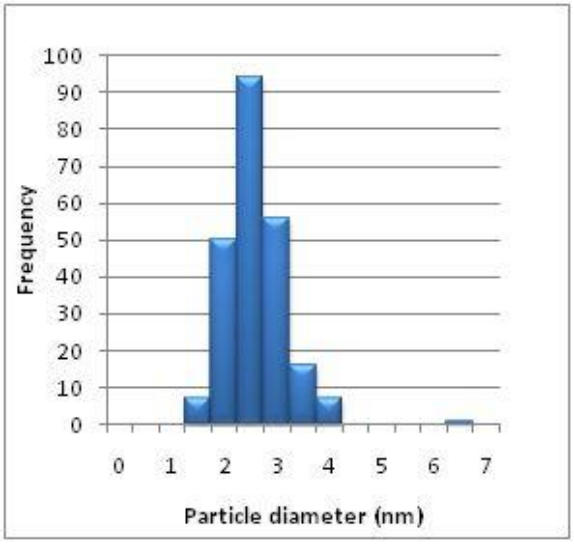

Particle Count	*Mean diameter (nm)*	*sdev (nm)*
232	2.4	0.8

Fig. S2: HR-TEM analysis of small methylphosphonate-stabilised gold nanoparticles

a

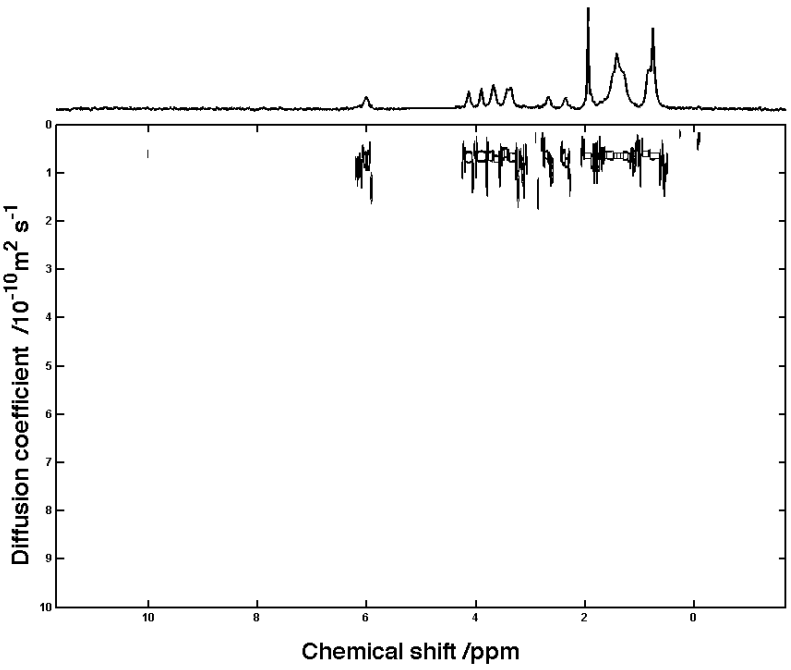

D: ~ 0.8 x 10^{-10} m^2 s^{-1}

R_H: ~ 3 nm

b

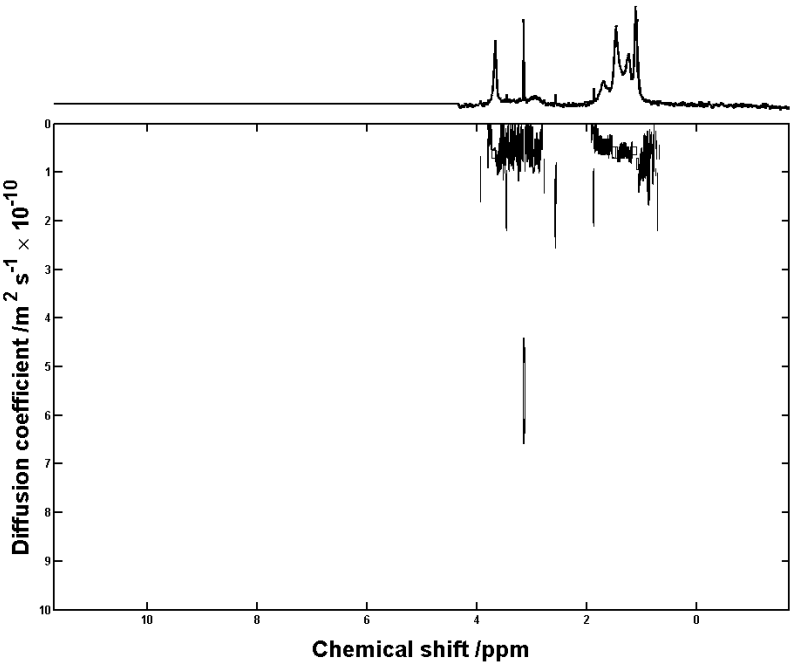

D: ~ 0.5 x 10^{-10} m^2 s^{-1}

R_H: ~ 5 nm

Fig. S3: DOSY-NMR spectra for "small TamiGold" (**a**) and small methylphosphonate-stabilised gold nanoparticles (**b**). Solvent: D_2O (solvent signal suppressed). For a calculation of the hydrodynamic radius R_H from the diffusion coefficient D see Suppl. Methods (p. 37).

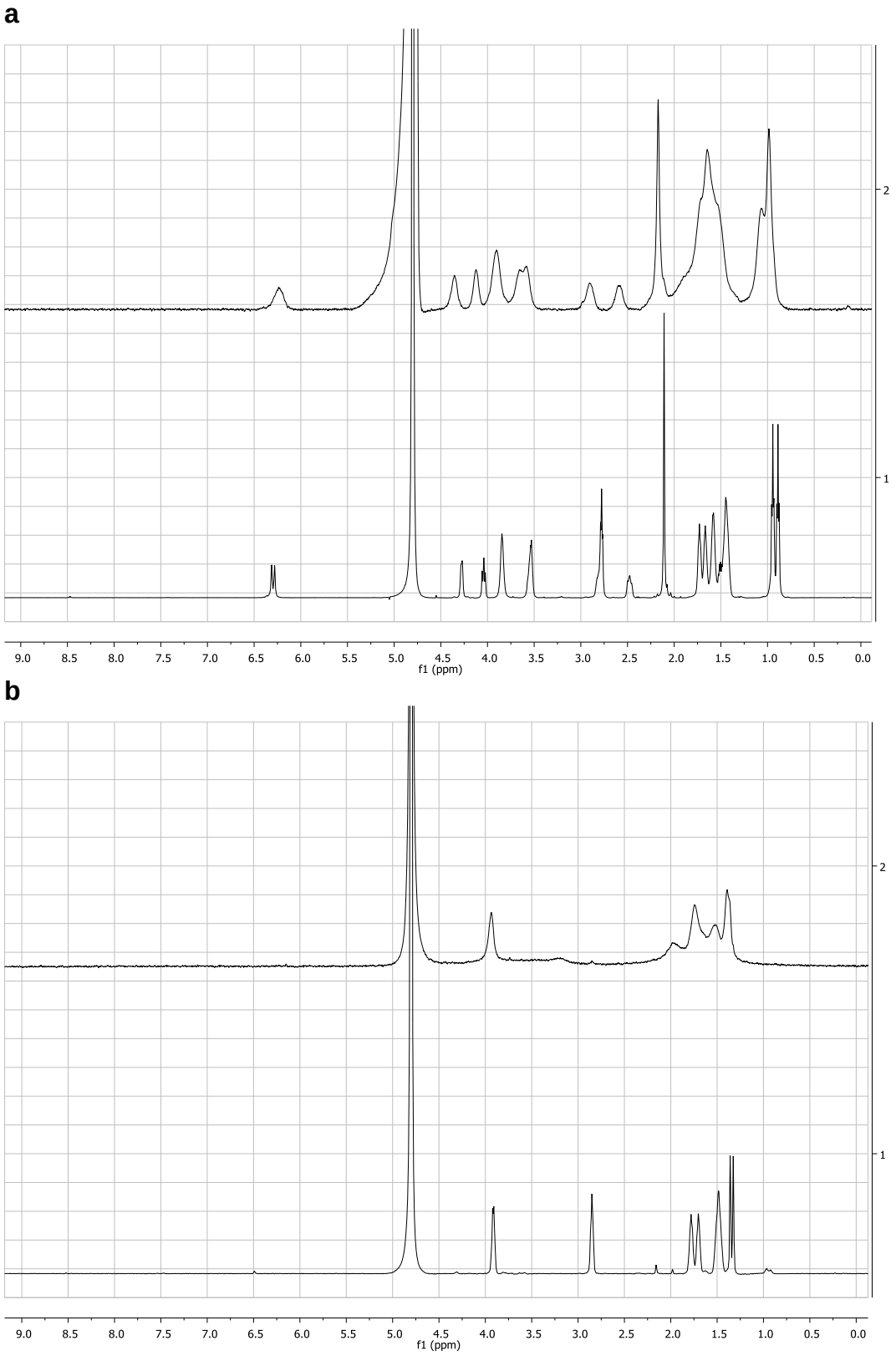

Fig. S4: (**a**) ^{1}H-NMR-spectra overlay of "small TamiGold" with **4.** (**b**) ^{1}H-NMR-spectra overlay of small methylphosphonate-stabilised gold nanoparticles with **13**. Solvent: D_2O. Line broadening of 1.5 Hz was applied to the nanoparticle spectra.

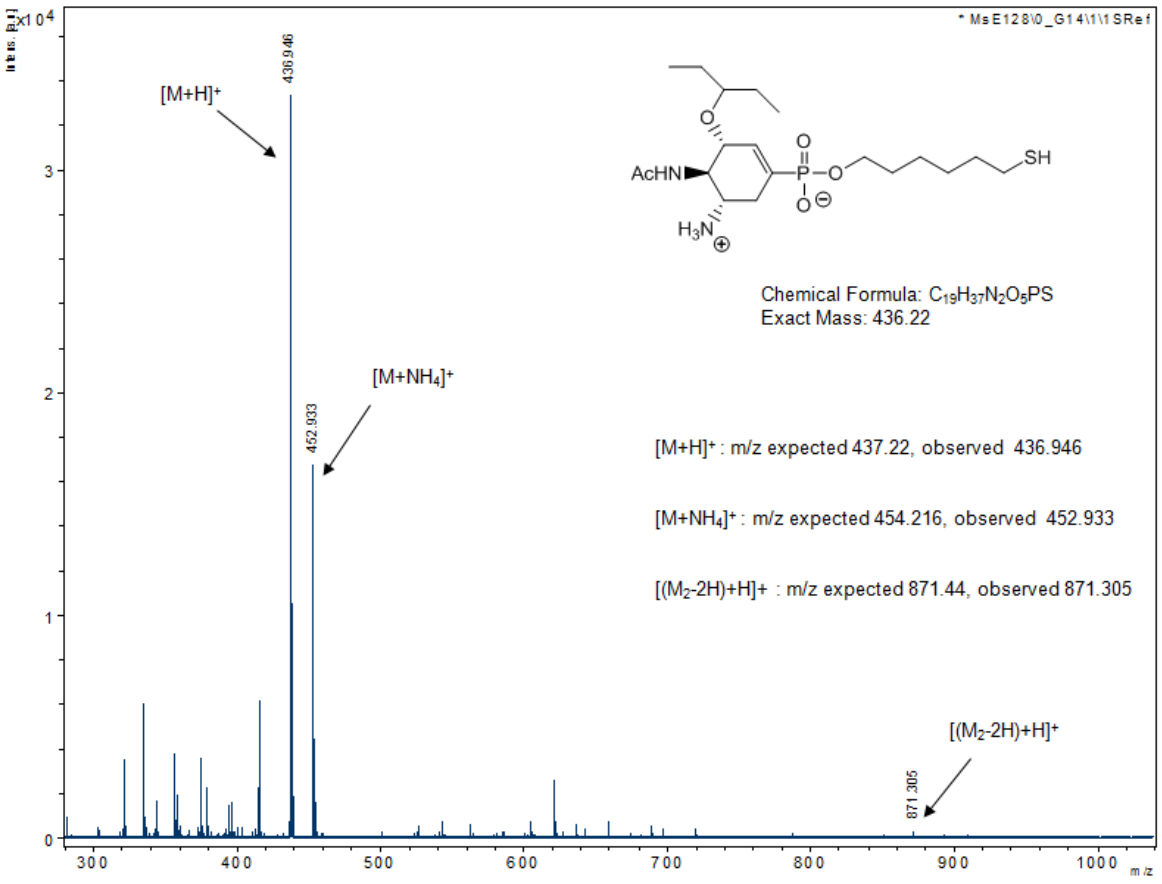

Fig. S5: MALDI-MS of “small TamiGold”. Fragmentation leads to detection of monomeric thiol ligand.

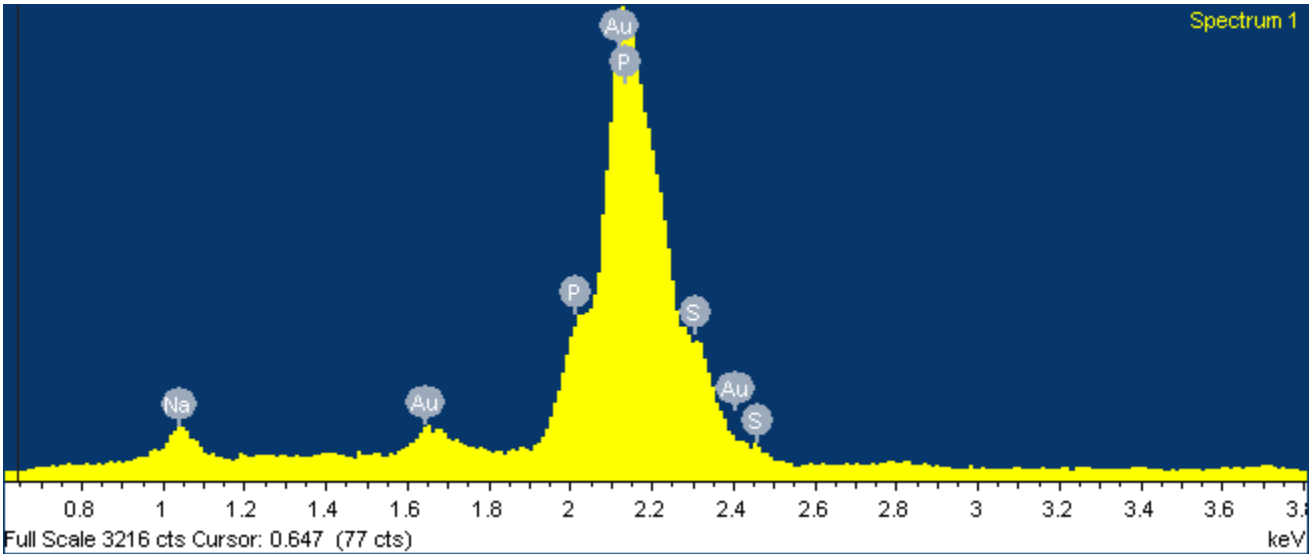

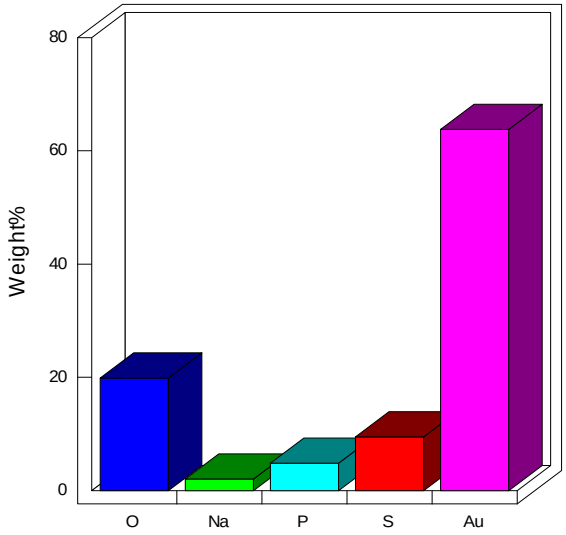

Fig. S6: EDX analysis of "small TamiGold", resulting in a Au/S ratio of approx. 1:1.

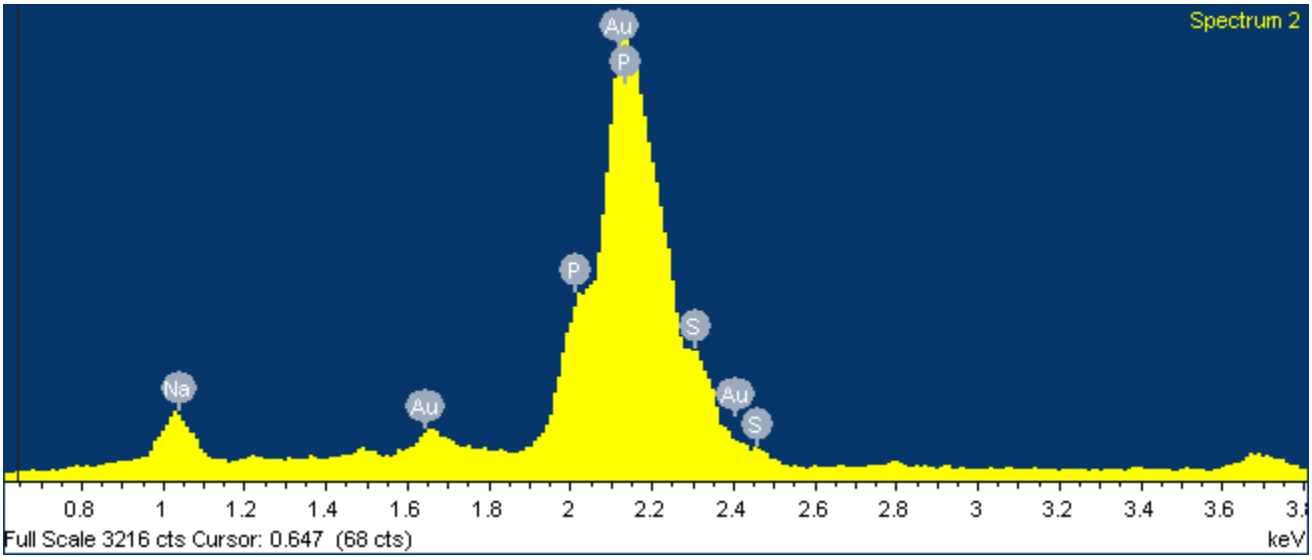

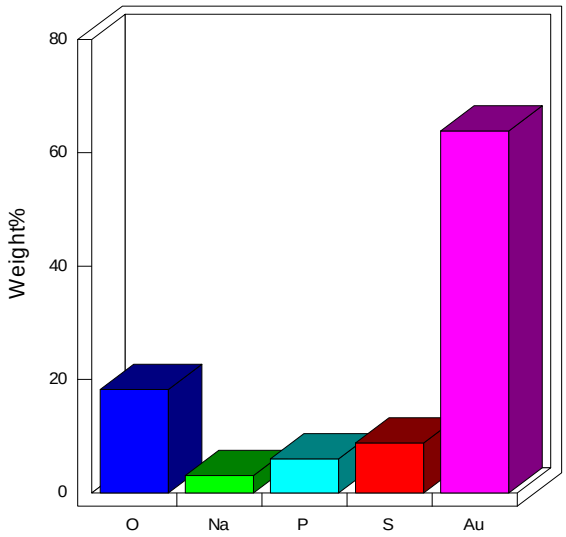

Fig. S7: EDX analysis of small methylphosphonate-stabilised gold nanoparticles (control), resulting in a Au/S ratio of approx. 1:1.

a

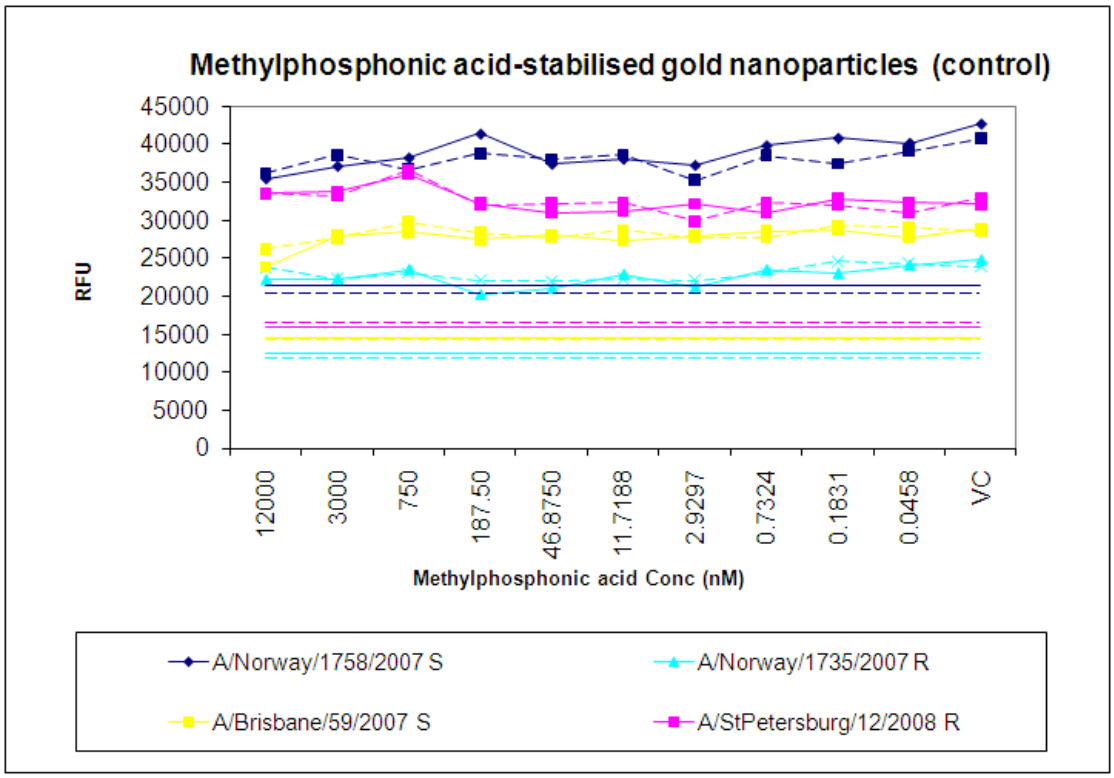

b

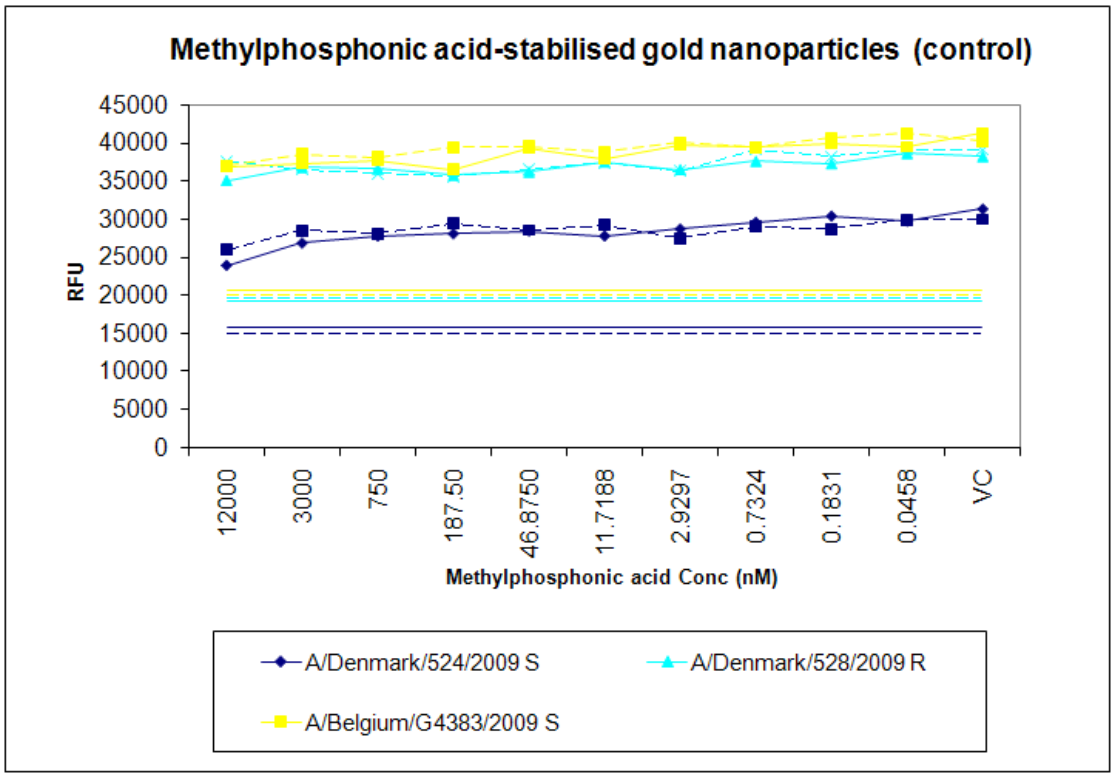

Fig S8: Inhibition of the neuraminidase activity of influenza virus strains (H1N1) by small methylphosphonate-stabilised gold nanoparticles. (**a**) Seasonal influenza virus strains (H1N1). (**b**) Pandemic influenza virus strains (H1N1). S = Oseltamivir-sensitive. R = Oseltamivir-resistant. VC = Virus only control. No inhibition was detected within the concentration range tested

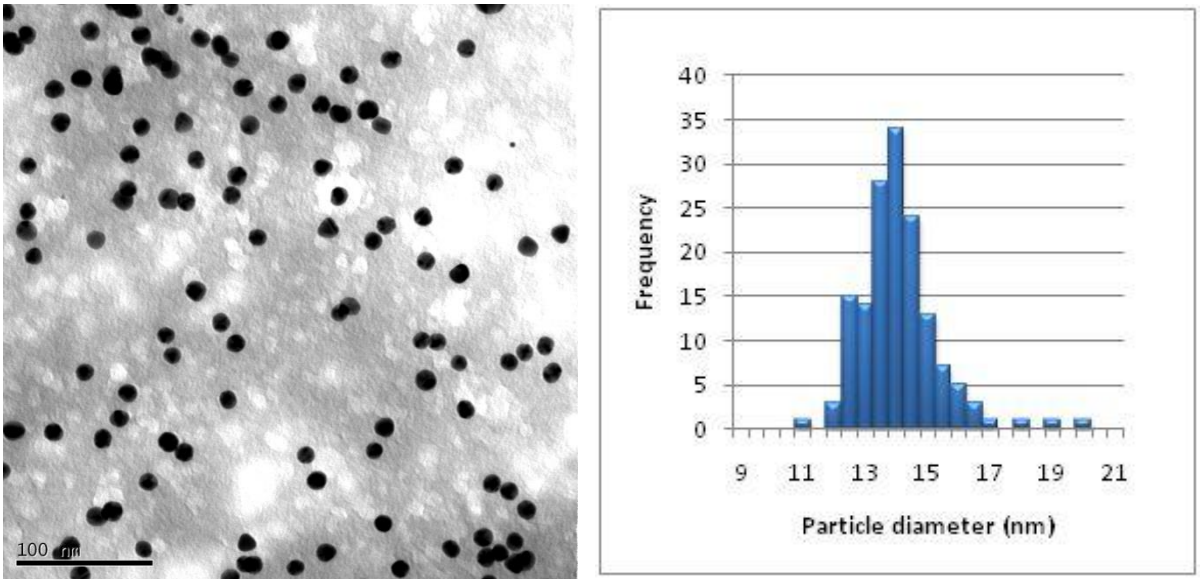

Particle Count	*Mean diameter (nm)*	*sdev (nm)*
151	13.9	1.2

Fig. S9: TEM analysis of large phospha-oseltamivir-stabilised gold nanoparticles ("large TamiGold")

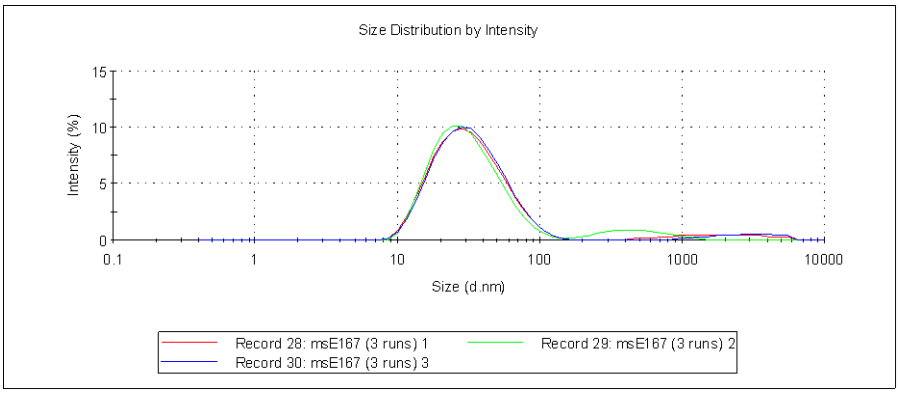

Size distribution (Intensity)

Diameter (nm):	34.9	(94 %)
	598.6	(3 %)
	2903	(3 %)

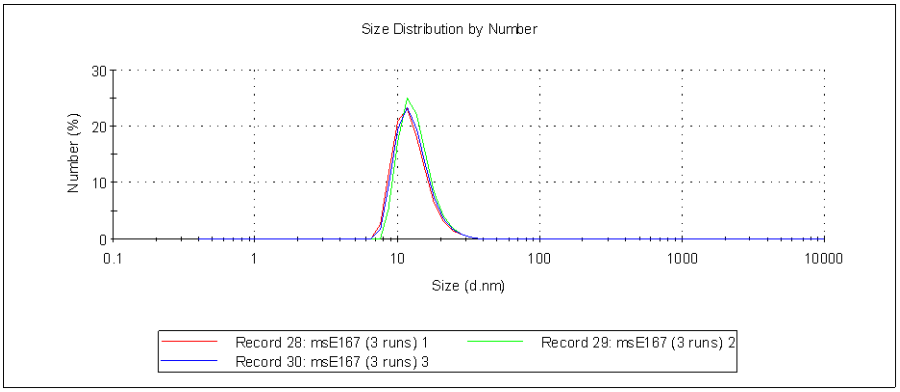

Size distribution (Number)

Diameter (nm):	13.2	(100 %)

Fig. S10: Dynamic light scattering analysis of “large TamiGold”, resulting in a number size distribution of 13.2 nm (diameter) and a Z-average diameter of 28.2 nm. (Polydispersity Index: 0.265)

a

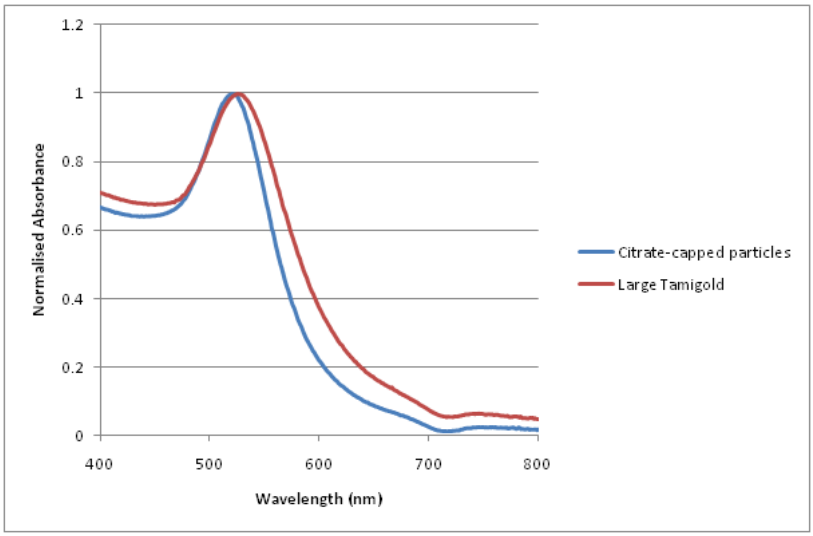

b

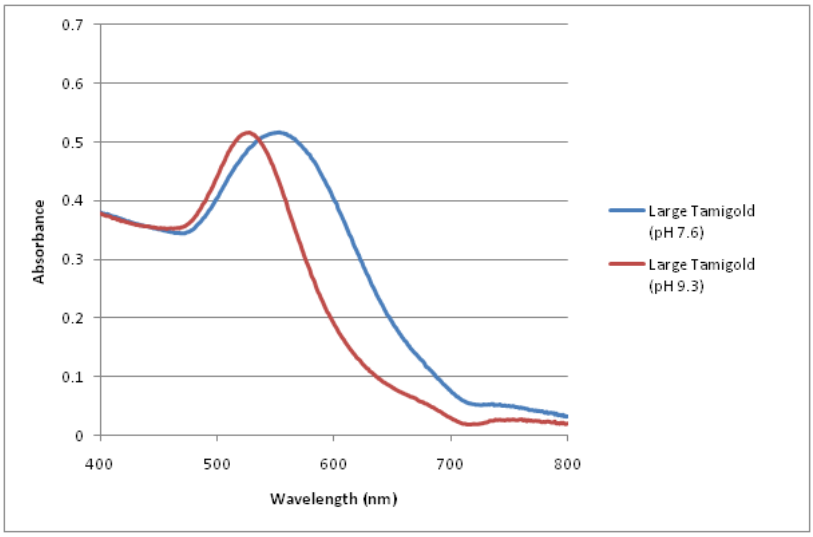

c

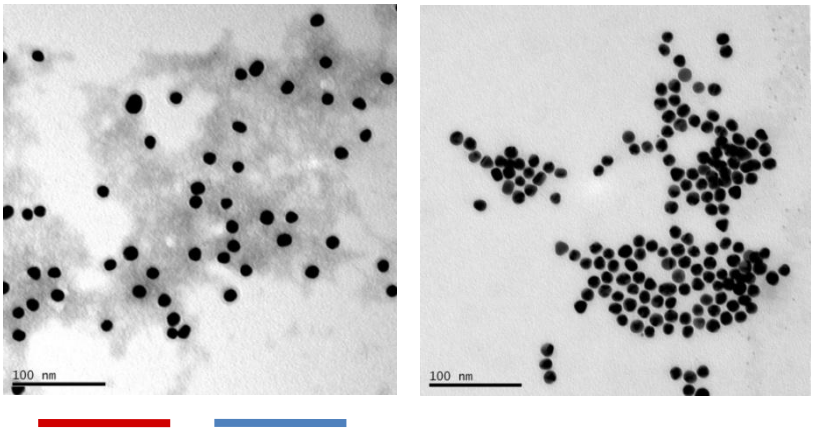

Fig. S11: **a**: Comparison of UV-VIS spectra of citrate-capped gold nanoparticles and "large TamiGold", obtained by ligand exchange, by compound **4**, of the former. **b**: Slow aggregation (over 3 days) of "large TamiGold" when dialysed against phosphate buffer at physiological pH (pH 7.6). **c**: TEM images before and after aggregation as described under **b**. See also Supplementary Discussion.

a

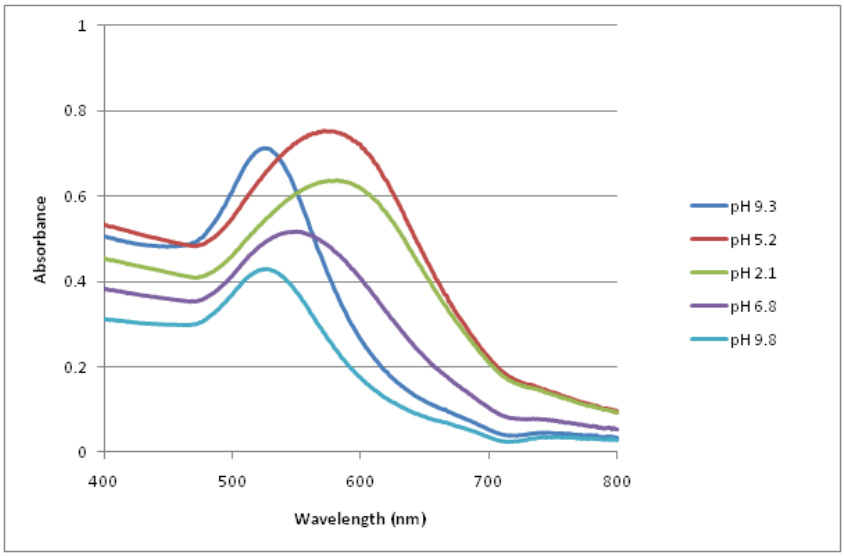

b

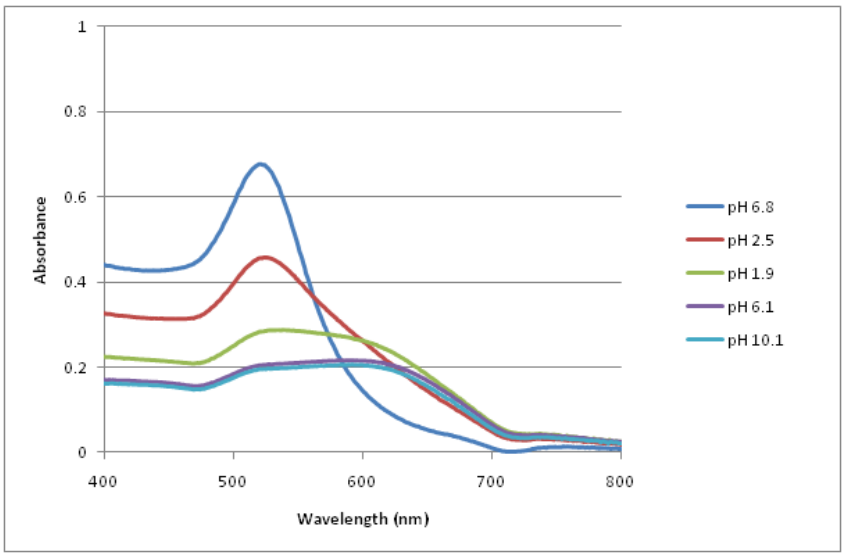

Fig. S12: (**a**) pH-dependant aggregation and resuspension of "large TamiGold". (**b**) Irreversible aggregation of citrate-capped gold nanoparticles under the same conditions

a

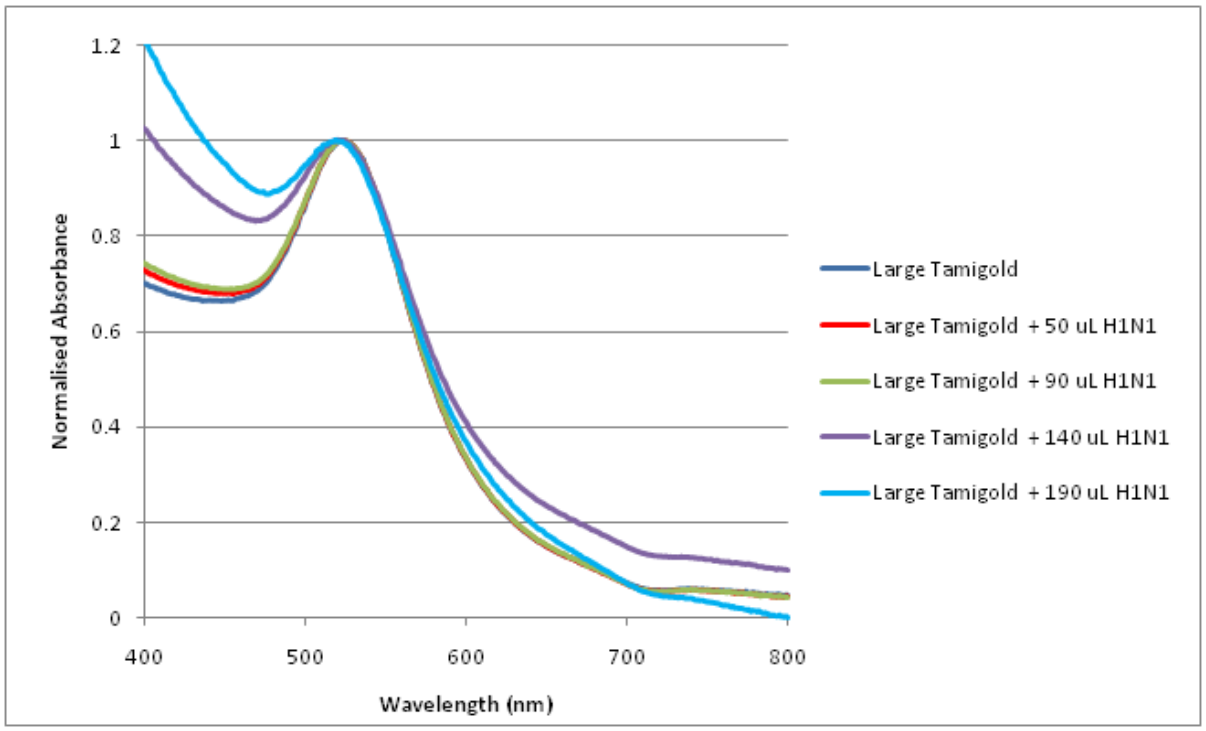

b

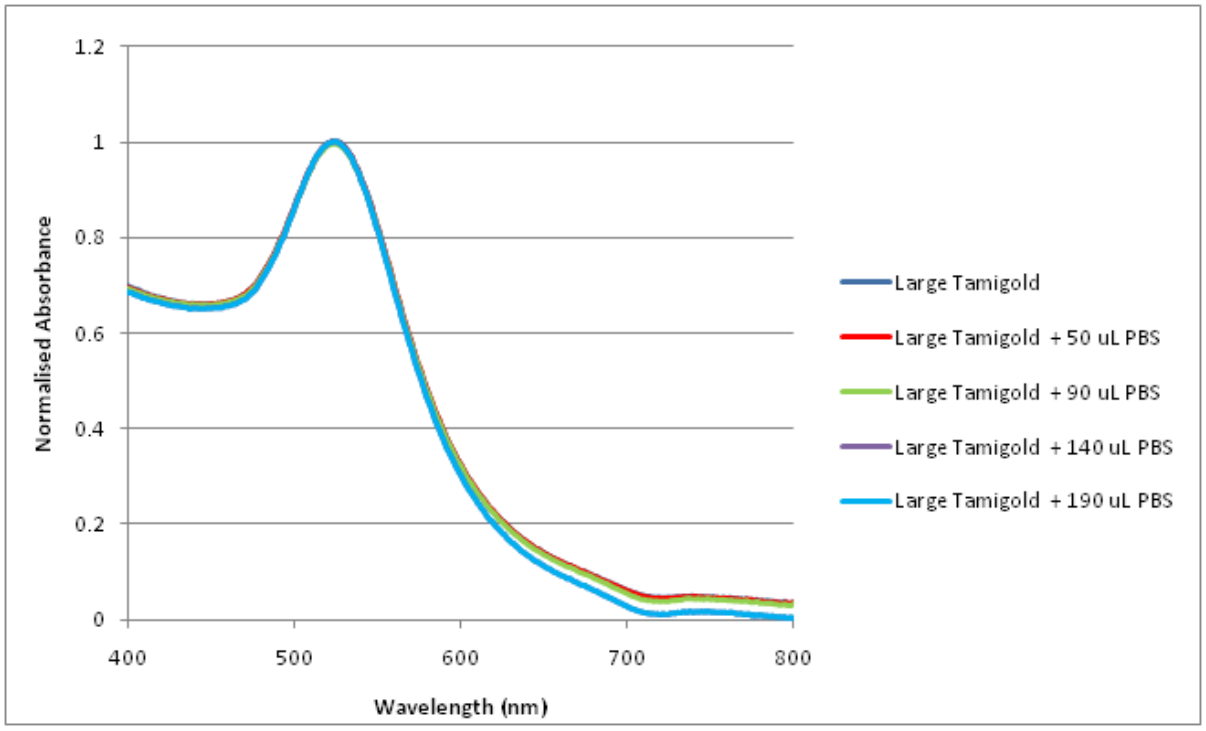

Fig. S13: (**a**) Addition of increasing amounts of influenza virus (PR8, 1mg/mL) to 'large TamiGold', resulting in a slight blueshift (~ 5 nm) of the absorption band. (**b**) Dilution of a solution of 'large TamiGold' (same concentration as under a) with buffer. No blueshift was observed under the latter conditions.

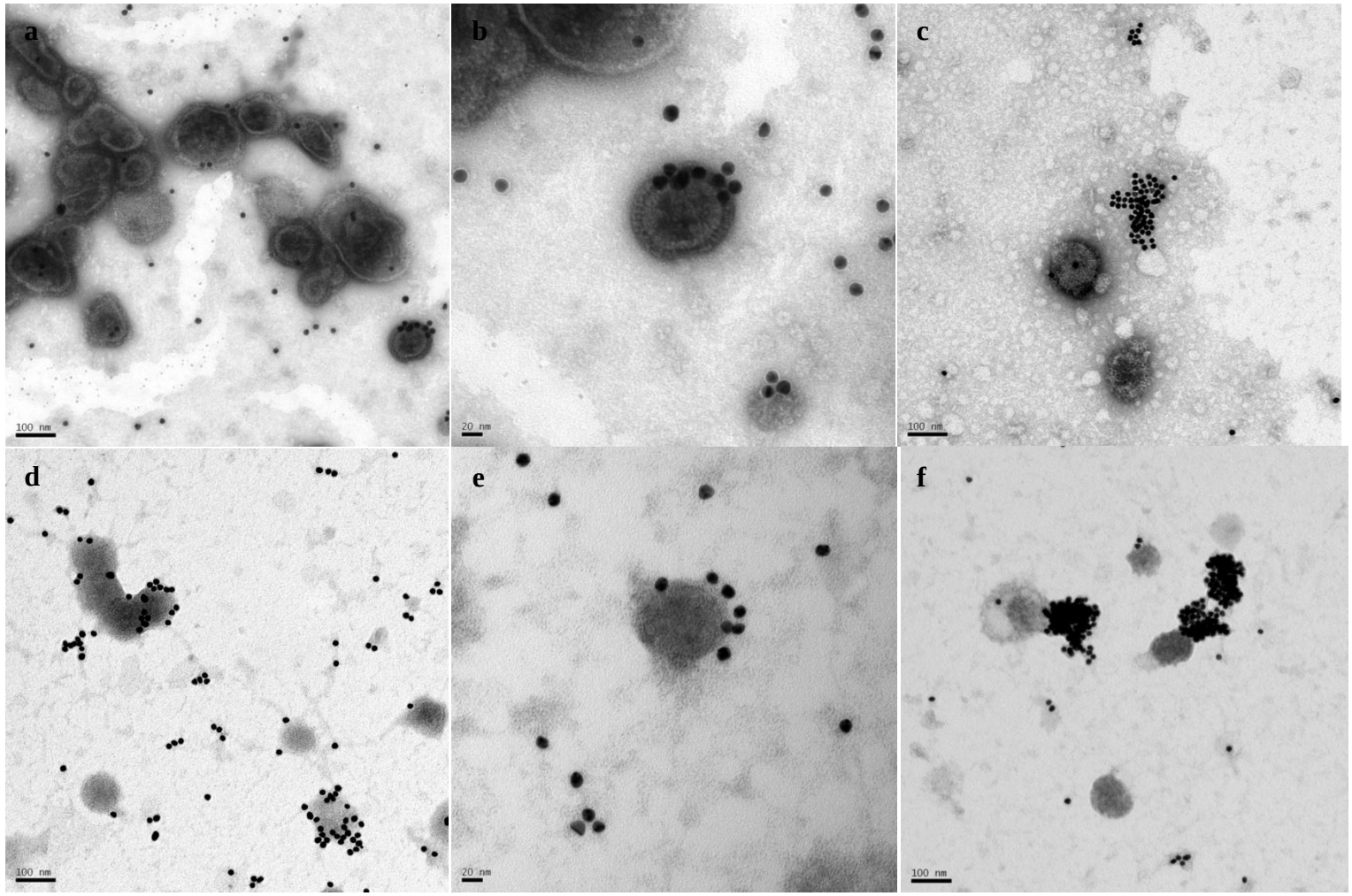

Fig. S14: **a-c**: Fig. 2 in communication. **d-f**: Another example of selective binding of "large TamiGold" to influenza virus. **d**, **e**: Clustering of "large TamiGold" on the virus surface. **f**: Aggregation of "large TamiGold" in presence of monomeric inhibitor (deprotected **3**).

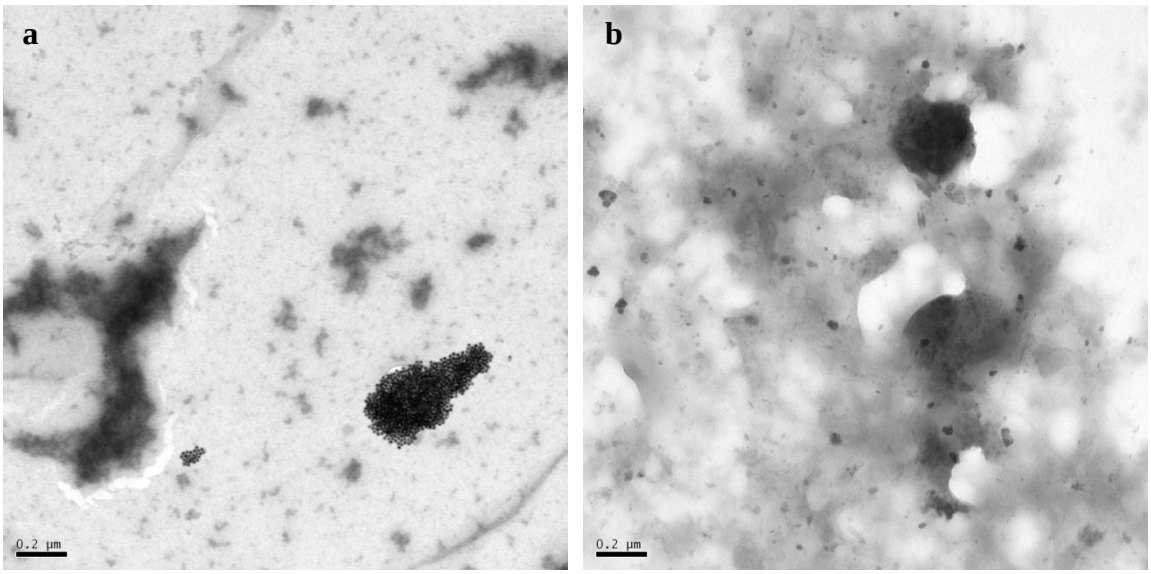

Fig. S15: **a**: Aggregation "large TamiGold" upon addition of inhibitor (deprotected **3**) in absence of virus. **b**: Blank grid + Tris buffer (10mM, pH9.3) + 2 % uranyl acetate (staining reagent..

Supplementary Discussion

1 Interaction with active site, pharmacophore, charge etc.

2 Determination of the particle size distribution of 'small TamiGold' and methylphosphonate-stabilised gold nanoparticles (control)

HR-TEM resulted in an average size of ~ 2 nm (1.97 nm) with size ranging from 1-4 nm. This finding was corroborated by DOSY-NMR, which gave a hydrodynamic radius of 3 nm (avg.).The larger diameter thus obtained by the DOSY-NMR method is due to it including the ligand shell and the hydration sphere of the respective nanoparticle. Consequently, HR-TEM-obtained values were used to calculate particle concentrations for inhibition studies.

The difference in size of small TamiGold' and methylphosphonate-stabilised gold nanoparticles (control) was slightly larger when investigated by DOSY-NMR (3 nm and 5 nm, respectively) than with HR-TEM (2 nm and 2.4 nm, respectively). This can be, for instance, explained by the different chemical nature of the terminating group (phospha-oseltamivir vs. methylphosphonate).

3 Under the conditions used, fragmentation of "small TamiGold" occurs and the molecular ion species $(M+H)^+$ of the monomeric thiol ligand is consequently detected as the peak with highest intensity. (Fig. S5)

4 EDX-analysis:

EDX confirmed the presence of Au, S and P as major constituents of the nanoparticles synthesised.

"Small TamiGold": 60% Au/10% S (% mass) results in a molar ratio of approx. 1:1.

A similar result is obtained for methylphosphonate-stabilised gold nanoparticles (control).

Similar values for small gold nanoparticles obtained by EDX have been reported.[3]

The Au/S ratio is likely to be an overestimate with respect to S due to peak overlap of the Au/S/P peaks. We estimate an associated error of 10-20%.[4]

5 The oseltamivir-resistant (R) influenza virus strains carry the well-documented H275Y mutation in the neuraminidase.[5]

6 Inhibition of seasonal and pandemic influenza virus strains assays by "small TamiGold" and methylphosphonate-stabilised gold nanoparticles (control)

In Fig. 2, 50% inhibition of influenza virus strain A/St. Petersburg/12/2008 was slightly outside the maximum particle concentration tested. The value given is an extrapolation of the data points obtained, clearly showing inhibition.
The main contributing factors to errors in the inhibitory concentrations of phospha-oseltamivir epitopes on "small TamiGold" arise from a) the fact that not all phospha-oseltamivir moieties on a given particle are available for binding, b) the error in the Au/S ratio determined by EDX (see above) and c) assumptions made regarding the morphology of gold nanoparticles (e. g. the spherical shape assumed for calculations of n_{Au}, see p. 39).

7 Oseltamivir carboxylate as the active ingredient of Tamiflu inhibits the NA of resistant influenza virus strains (carrying the H274Y mutation) by a factor of 10^2 - 10^3 weaker than the NA from oseltamivir-sensitive strains.[5]

8 Determination of the particle size distribution of 'large TamiGold' by TEM and DLS
DLS gave a Z-average diameter of 28.2 nm and a number average particle size of 13.2 nm. This is in good agreement with the TEM-derived average particle size of 14 nm (13.9 ± 1.2 nm, size distribution: 12-17 nm) (Fig.S9 and S10).

9 Effect of pH and virus on the surface plasmon band of "large TamiGold".
Ligand exchange of citrate-capped (Turkevitch) particles by **4** resulted in a redshift of absorption from 519 nm (citrate-capped) to 525 nm ("large TamiGold"). (Fig. S11a) The SPR-absorption of "large TamiGold" undergoes a significant redshift and band broadening in the physical pH-range from 525 nm (pH 9.3) to 553 nm (pH 7.6) which was entirely reversible when pH was adjusted to > 9 (Fig. S11b and c). This red shift is indicative of a reduction in the inter-particle distance (see TEM images Fig. S11c) which shifts the absorbance to lower energies.[6-8]

Such behaviour is characteristic for particles stabilised with cationic groups on the surface but not for the citrate-capped (Turkevitch) particles where pH-decrease resulted in irreversible aggregation (Fig. S12a and b). This represents another confirmation of the change in surface functionalisation from citrate to phospha- oseltamivir.

10 A qualitative assessment of the effect of virus on the wavelength of the surface plasmon band was carried out. Addition of increasing amounts of virus resulted in a slight blueshift of the absorption band (see Fig. S13) which was not observed when a virus-free sample was diluted. Whether this is due to virus binding, molecular crowding or -decrowding effects remains to be investigated in more detail.

Supplementary Methods

General

Reaction solvents were purchased anhydrous and used as received. Solvents for chromatography were distilled before use. Reactions were monitored by TLC using precoated silica gel 60 F_{254} plates. Compounds were detected by UV absorption and/or by staining with a molybdenum phosphate reagent (20 g ammonium molybdate and 0.4 g cerium(IV) sulfate in 400 mL of 10% aq. sulfuric acid) or a basic $KMnO_4$-solution and subsequent heating at 120 °C for 5 min. Silica gel 60 A 'Davisil' (particle size 35-70 μm) from Fisher Scientific, UK and silica gel 100 C18 reversed phase (particle size 40-63 μm) from Fluka Analytical, UK were used for flash chromatography. ^{1}H NMR, ^{13}C NMR, ^{31}P NMR and all multidimensional NMR spectra were recorded on Varian VNMRS spectrometers (600 MHz, 500 MHz or 400 MHz, see compound characterisation for individual experiments). Chemical shifts in ^{1}H NMR and ^{13}C NMR spectra were referenced to the residual proton resonance of the respective deuterated solvent, $CDCl_3$ (7.26 ppm), D_2O (4.80 ppm), CD_3OD (3.31 ppm). For ^{31}P NMR spectra H_3PO_4 was used as external standard (0 ppm). In some cases, ^{13}C chemical shifts were deduced from heteronuclear multiple spin correlation (HSQC) spectra. The H-6_{ax} and H-6_{eq} assignments refer to the pseudoaxial and pseudoequatorial protons in the cyclohexene systems, respectively, obtained by ROESY spectroscopy. HR-ESI MS spectra were recorded on a Bruker Daltonics Apex III in positive mode with MeOH/H_2O as solvent. MALDI-MS spectra were recorded using cyanohydroxycinnamic acid (CHCA) or dihydroxybenzoic acid (DHB) as matrix. Fluorescence was measured in a JASCO FP-6300 fluorimeter. Silica-based MPLC chromatography was carried out on the Büchi Sepacore system equipped with glass columns packed with LiChroprep Si 60 (15-25 μm) from Merck, Darmstadt, Germany. Gel permeation chromatography was carried out in the 1-10 mg scale on a XK 16/70 column (bed volume 130 mL), from Amersham packed with Sephadex G-10 (particle size 40-120 μm) and 0.1 M NH_4HCO_3 as buffer. Detection was achieved with a differential refractometer from Knauer, Berlin, Germany. pH values of gold nanoparticle solutions were recorded with a Hanna Instruments pH 209 meter (unless otherwise stated) calibrated between pH 7 and pH 10. Fine chemicals were purchased from Aldrich-, Sigma- or Acros-Chemicals and were of the highest purity available. Abbreviations: THF (tetrahydrofuran), TIPS (trisiopropylsilyl), EA (ethyl acetate), Tol (toluene), TFA (trifluoroacetic acid), TBAF (tetrabutylammonium fluoride), DMAP (*p*-dimethylaminopyridine), DMF (dimethyl formamide), DE (diethyl ether), DCM

(dichloromethane), AcOH (acetic acid), MeOH (methanol), TLC (thin layer chromatography).

Small Molecule Syntheses

Ammonium [methyl (3*R*,4*R*,5*S*)-4-acetamido-5-(1,1-dimethylethyloxycarbonylamino)-3-(1-ethylpropoxy)-1-cyclohexene-1-phosphonate] (3)

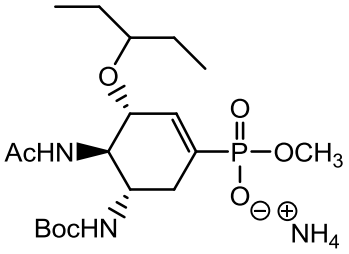

Monoester **(3)** was synthesised from the 'acetamido-azide' precursor as published previously.[9]

6',6'-Dithiobis (hex-1'-yl [(*3R,4R,5S*)-4-acetamido-5-amino-3-(1-ethylpropoxy)-1-cyclohexene-1-phosphonic acid]) (4)

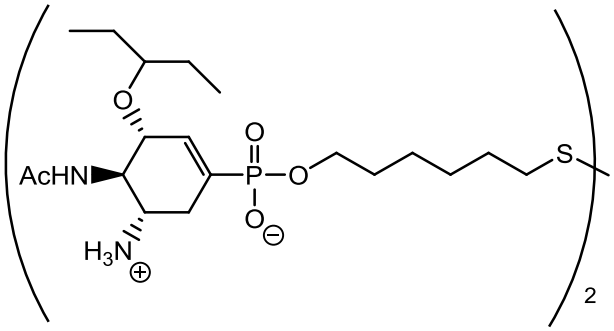

Compound **(6)** (8.2 mg, 0.00746 mmol) and NaI (4.9 mg, 0.0328 mmol) was placed under an N_2 (g) atmosphere in a reflux condenser and dissolved in dry acetone (1.5mL). The solution was heated to reflux for 8 hour periods over 3 days, with the addition of a further 2 portions of NaI (4.9 mg, 0.0328 mmol) and acetone to maintain the original volume. Once TLC analysis confirmed the reaction was complete, the solvent was evaporate *in vacuo* and the residue was purified by flash chromatography (EA:MeOH; 5:1 → 2:1 → 1:1 → MeOH) to yield the desired monophosphonate intermediate (6.5mg, 80%). The residue was then treated with dioxane (0.5 mL) and 50% TFA/H_2O (0.5 mL) for 36 hours. The solvent was then evaporated *in vacuo* and the residue was purified by gel permeation chromatography to afford compound **(4)** (5.7 mg, 90%).

^{1}H NMR (600 MHz, D_2O) δ_H: 0.92 (6 H, 2t, J = 7.1, 7.3 Hz, -OCH(CH_2CH_3)$_2$), 1.38 – 1.53 (4 H, m, -$CH_2CH_2CH_2CH_2$S-), 1.54 – 1.62 (4 H, m, -OCH(CH_2CH_3)$_2$), 1.67 (2 H, m, -OCH_2CH_2-), 1.73 (2 H, m, -SCH_2CH_2-), 2.11 (3 H, s, -NHCOCH_3), 2.48 (1 H, dd, J = 12.0, 13.3 Hz, H_{6ax}), 2.78 (1 H, dd, J = 7.0, 7.0 Hz, -SCH_2-), 2.77 – 2.84 (1 H, m, H_{6eq}), 3.50 – 3.60 (2 H, m, H_5, -OCH(CH_2CH_3)$_2$), 3.85 (2 H, m, -OCH_2-), 4.04 (1 H, dd, J = 10.0, 10.2 Hz, H_4), 4.28 (1 H, d, J = 6.9 Hz, H_3), 6.30 (1 H, d, J_{P-2} = 19.3 Hz, H_2);
^{13}C NMR (150.8 MHz, D_2O) δ_C: 8.63, 8.91 (-OCH(CH_2CH_3)$_2$), 22.36 (-NHCOCH_3), 24.91, 25.26, 25.70, 27.57 (-$CH_2CH_2CH_2CH_2$S-, -OCH(CH_2CH_3)$_2$), 28.50 (-SCH_2CH_2-), 29.55 (m, C6), ~30.00 (d, J = 6.7 Hz, -OCH_2CH_2-), 38.38 (-SCH_2-), ~49.59 (d, J = 14.7 Hz, C5), 53.24 (C4), 65.27 (-OCH_2-), ~75.89 (1 H, d, J = 18.2 Hz, C3), 83.71 (-OCH(CH_2CH_3)$_2$), ~130.43 (1 H, d, J_{P-1} = 173 Hz, C1), 135.17 (m, C2), 174.91 (-NHCOCH$_3$);
^{31}P NMR (242.7 MHz, D_2O) δ_P: 12.33 (s).
HR-ESI-MS (m/z) calculated for $C_{38}H_{72}N_4O_{10}P_2S_2$ $(M+Na)^+$ 893.4057, found 893.4084.

(6'-Acetylthiohex-1'-yl) methyl [(*3R,4R,5S*)-4-acetamido-5-(1,1 dimethylethyloxycarbonylamino)-3-(1-ethylpropoxy)-1-cyclohexene-1-phosphonate] (5)

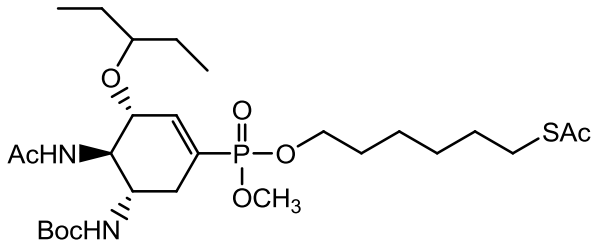

Compound **(10)** (49 mg, 0.177 mmol) was placed under an N_2 (g) atmosphere and dry acetonitrile (1.5 mL) was added. (**3**) (70 mg, 0.131 mmol), previously lyophilised with NEt_3 (1 eq.) was then quickly added to the stirring solution. After stirring overnight, TLC analysis indicated the reaction had not progressed any further and that triflate **(10)** had degraded in solution. The solvent was evaporated *in vacuo* and the residue was directly purified by flash chromatography (Tol:EA; 1:1 → EA → EA:MeOH; 5:1→MeOH) to give compound **(5)** (31 mg, 71% based on recovered starting material). R_f: 0.51 (EA).
^{1}H NMR (500 MHz, $CDCl_3$) δ_H: 0.86 (6 H, m, -OCH(CH_2CH_3)$_2$), 1.37 (4 H, m, -$CH_2CH_2CH_2CH_2$S-), 1.40 (9 H, s, -NHCOC(CH_3)$_3$), 1.48 (4 H, m, -OCH(CH_2CH_3)$_2$), 1.56 (2 H, m, -SCH_2CH_2-), 1.64 (2 H, m, -OCH_2CH_2-), 1.96 (3 H, s, -NHCOCH_3), 2.20 (1 H, m,

H_{6ax}), 2.30 (3 H, m, -SCOC$\underline{H}_3$), 2.59 (1 H, m, H_{6eq}), 2.85 (2 H, dd, J = 1.4, 7.8 Hz, -SC$\underline{H}_2$-), 3.33 (1 H, m, -OC$\underline{H}$(CH_2CH_3)$_2$), 3.68 (3 H, 2d, J = 11.0 Hz, P-OC$\underline{H}_3$), 3.78 (1 H, m, H_5), 3.88 – 4.09 (4 H, m, -OC$\underline{H}_2$-, H_3, H_4), 5.16 (1 H, dd, J = 8.8, 9.3 Hz, -N$\underline{H}$COCH_3), 5.88 (1 H, d, J = 9.2 Hz, -N$\underline{H}$COC(CH_3)$_3$), 6.58 (1 H, d, $J_{P\text{-}2}$ = 22.1 Hz, H_2);

^{13}C NMR (100.5 MHz, $CDCl_3$) δ_C: 9.25, 9.67 (-OCH($CH_2\underline{C}H_3$)$_2$), 23.45 (-NHCO$\underline{C}H_3$), 25.16, 26.22 (-$\underline{C}H_2\underline{C}H_2CH_2CH_2$S-), 25.70 (-OCH($\underline{C}H_2CH_3$)$_2$), 28.32, 28.35, 28.45 (-NHCOC($\underline{C}H_3$)$_3$), 29.02, 29.05 (-S$\underline{C}H_2$-), 29.49 (-SCH$_2\underline{C}H_2$-), 30.38 (m, -OCH$_2\underline{C}H_2$-), 30.74 (-SCOC$\underline{H}_3$), ~31.31 (m, C6), ~49.29 (m, C5), 52.54, 52.64 (2d, J = 5.3, 5.8 Hz, P-OC$\underline{H}_3$), 54.55 (m, C4), ~66.10 (2d, J = 5.8, 6.1 Hz, P-OC$\underline{H}_3$), ~76.32 (m, C3), 79.89 (-NHCO$\underline{C}$(CH_3)$_3$), 82.27 (-O$\underline{C}$H(CH_2CH_3)$_2$), ~126.93 (d, $J_{P\text{-}1}$ = 182 Hz, C1), 142.15 (m, C2), 156.36, 156.41 (-NH$\underline{C}$OC(CH_3)$_3$), 174.91 (-NH$\underline{C}$OCH_3), 196.14 (-S$\underline{C}$OCH_3);

^{31}P NMR (161.7 MHz, $CDCl_3$) δ_P: 18.28 (s).

HR-ESI-MS (m/z) calculated for $C_{27}H_{49}N_2O_8PS$ $(M+Na)^+$ 615.2839, found 615.2837.

6',6'-Dithiobis (hex-1'-yl methyl [(*3R,4R,5S*)-4-acetamido-5-(1,1 dimethylethyloxycarbonylamino)-3-(1-ethylpropoxy)-1-cyclohexene-1-phosphonate]) (6)

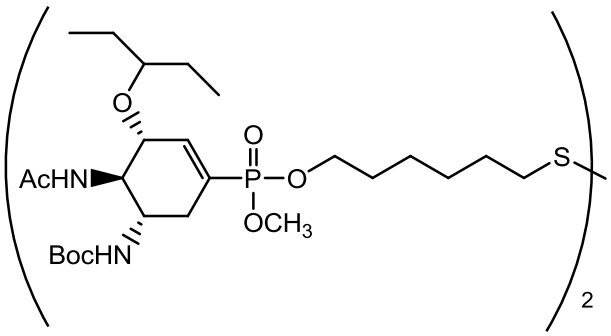

Compound **(5)** (28 mg, 0.0472 mmol) was placed under an O_2 (g) atmosphere and was dissolved in anhydrous MeOH (3.5mL). A methanolic NaOMe solution (~350 µL, 0.1M) was then added dropwise to the stirring solution of compound **(5)**, ensuring that the O_2 (g) was bubbling through the solution and that indicator paper indicated a pH ~ 10. After stirring overnight, the solvent was evaporated *in vacuo* and the residue was directly purified by flash chromatography (EA:MeOH; 10:1) to give compound **(X)** (16 mg, 60%). R_f : 0.71 (EA:MeOH; 5:1).

^{1}H NMR (500 MHz, $CDCl_3$) δ_H: 0.88 (m, 6H, -OCH($CH_2C\underline{H}_3$)$_2$), 1.42 (s, 13H, (-NHCOC($\underline{C}H_3$)$_3$, -OCH$_2$CH$_2$C$\underline{H}_2\underline{C}H_2CH_2CH_2$S-), 1.46 – 1.55 (m, 4H, -OCH($C\underline{H}_2CH_3$)$_2$), 1.64

– 1.73 (m, 4H, -OCH$_2$CH$_2$-, -SCH$_2$CH$_2$-), 1.98 (s, 3H, -NHCOCH$_3$), 2.22 (m, 1H, H$_{6ax}$), 2.60 (m, 1H, H$_{6eq}$), 2.68 (dd, 2H, J = 7.2, 7.5 Hz, -CH$_2$SAc), 3.34 (m, 1H, -OCH(CH$_2$CH$_3$)$_2$), 3.70 (d, 3H, J = 10.9 Hz, P-OCH$_3$), 3.80 (m, 1H, H$_5$), 3.93 (m, 1H, H$_7$), 4.02 (m, 3H, H4, -OCH$_2$-), 5.10 - 5.25 (m, 1H, -NH COCH$_3$), 5.82 - 5.94 (m, 1H, -NHCOCH$_3$), 6.60 (d, 1H, J_{P-2} = 21.8 Hz, H$_2$).

^{13}C NMR (100.5 MHz, CDCl$_3$) δ_C: 9.29, 9.73 (-OCH(CH$_2$CH$_3$)$_2$), 23.52 (-NHCOCH$_3$), 25.31, 25.72, 26.34 (-OCH(CH$_2$CH$_3$)$_2$, -OCH$_2$CH$_2$CH$_2$CH$_2$CH$_2$CH$_2$S-), 28.13, 28.48 29.15 (-NHCOC(CH$_3$)$_3$), 30.50 (m, -OCH$_2$CH$_2$-, -SCH$_2$CH$_2$-), ~31.37 (m, C6), 39.04, 39.10 (-CH$_2$S-), 49.31 (C5), 52.67 (2d, J = 5.5, 5.5 Hz, P-OCH$_3$), 54.64 (C4), 66.13 (m, -OCH$_2$-), 76.36 (m, C3), 79.86 (-NHCOC(CH$_3$)$_3$), 82.33 (-OCH(CH$_2$CH$_3$)$_2$), ~ 126.87 (d, J_{P-1} = 182 Hz, C1), 142.23 (m, C2), 156.44 (-NHCOC(CH$_3$)$_3$), 171.00 (-NHCOCH$_3$).

^{31}P NMR (161.7 MHz, CDCl$_3$) δ_P: 18.28 (s), 18.32 (s).

HR-ESI-MS (m/z) calculated for $C_{50}H_{92}N_4O_{14}P_2S_2$ $(M+Na)^+$ 1121.5419, found 1121.5437.

_O_-Toluenesulfonyl-_O_-triisopropylsilylhexane-1,6-diol (7)

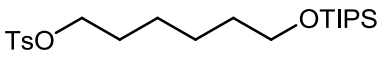

Hexane-1.6-diol was monosilylated with TIPSCl and imidazole in DCM as described in the literature.[1] Under an atmosphere of dry nitrogen, the product (3.86 g, 14.06 mmol) was dissolved in dry pyridine (12 mL). DMAP (172 mg, 1.41 mmol) and *p*-toluenesulfonyl chloride (4.02 g, 21.09 mmol) were added to the solution and the mixture stirred a 0°C for 4 hours. The reaction was quenched by addition of saturated aqueous NH_4Cl (5 mL). After evaporation to dryness, the residue was dissolved in DCM (15 mL) which was then extracted with NH_4Cl (5 mL), washed with brine (2x5 mL), the organic phase was dried over $MgSO_4$ and the solvent evaporated. Purification by flash chromatography (cyclohexane/DE; 10:1) gave compound **(7)** (4.79 g, 80%) as a clear oil. R_f : 0.27 (cyclohexane/DE; 10:1).).

^{1}H NMR (500 MHz, CDCl$_3$) δ_H: 1.00-1.10 (21 H, m, -Si(CH(CH$_3$)$_2$)$_3$, -Si(CH(CH$_3$)$_2$)$_3$), 1.27 – 1.35 (4 H, m, HOCH$_2$CH$_2$CH$_2$CH$_2$-), 1.48 (2 H, m, -CH$_2$CH$_2$OSi-), 1.64 (2 H, m, -CH$_2$CH$_2$OTs), 2.44 (3 H, s, H$_3$C-Ph-), 3.63 (2 H, t, J = 6.4 Hz, -CH$_2$OSi), 4.02 (2 H, t, J = 6.4, 6.5 Hz, Ts-OCH$_2$-), 7.33 (2 H, d, J = 8.0 Hz, H$_{Aryl}$), 7.78 (2 H, d, J = 8.1 Hz, H$_{Aryl}$);

^{13}C NMR (150.9 MHz, CDCl$_3$) δ_C: 12.15 (-Si(CH(CH$_3$)$_2$)$_3$), 18.16 (-Si(CH(CH$_3$)$_2$)$_3$), 21.73 (CH$_3$-Ph-), 25.36, 25.40 (TsOCH$_2$CH$_2$CH$_2$CH$_2$CH$_2$CH$_2$O-), 29.01, 32.86

(TsOCH$_2$CH$_2$CH$_2$CH$_2$CH$_2$CH$_2$O-), 63.31 (-CH$_2$OSi),70.75 (TsOCH$_2$-), 128.00, 129.91 (CH$_{Aryl}$), 133.50, 144.71 (C$_{Aryl}$);
HR-ESI-MS (m/z) calculated for $C_{22}H_{40}O_4SSi$ $(M+Na)^+$ 451.2309, found 451.2306.

6-Triisopropylsilyloxy-*S*-acetyl-hexan-1-thiol (8)

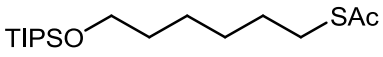

Compound **(7)** (4.792 g, 0.011 mol) was dissolved in pyridine (65 mL), then KSAc (3.83 g, 0.033 mol) was added to the solution. The mixture was stirred for 5 hours at room temperature. Pyridine was removed under high vacuum and the residue was dissolved in DCM (50 mL). The solution was washed with saturated aqueous NH_4Cl (2x15 mL), NaCl (20 mL), the organic phase was dried over $MgSO_4$ and the solvent evaporated. Purification by flash chromatography (Tol) afforded compound **(8)** (3.208 g, 86%) as an clear oil. R_f : 0.46 (Tol).
^{1}H NMR (500 MHz, $CDCl_3$) δ_H: 1.02 – 1.12 (21 H, s, -Si(CH(CH$_3$)$_2$)$_3$), -Si(CH(CH$_3$)$_2$)$_3$), 1.37 (4 H, m, -CH$_2$CH$_2$CH$_2$CH$_2$S-), 1.50 – 1.62 (4 H, m, -OCH$_2$CH$_2$-, -SCH$_2$CH$_2$-), 2.32 (3 H, s, -SCOCH$_3$), 2.87 (2 H, t, J = 6.9, 7.1 Hz, -SCH$_2$-), 3.67 (2 H, t, J = 6.2, 6.3 Hz, -OCH$_2$-);
^{13}C NMR (150.9 MHz, $CDCl_3$) δ_C: 12.20 (-Si(CH(CH$_3$)$_2$)$_3$), 18.20 (-Si(CH(CH$_3$)$_2$)$_3$), 25.56, 28.82 (-CH$_2$CH$_2$CH$_2$CH$_2$S-), 29.29 (-CH$_2$S-), 29.88 (-CH$_2$CH$_2$S-), 30.77 (-SCOCH$_3$), 33.00 (-CH$_2$CH$_2$O-), 63.47 (-CH$_2$O-);
HR-ESI-MS (m/z) calculated for : $C_{17}H_{36}O_2SSi$ $(M+Na)^+$ 355.2097, found 355.2091.

6-Hydroxy-*S*-acetyl-hexan-1-thiol (9)

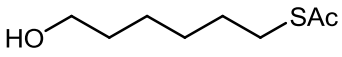

Compound **(8)** (0.874 g, 2.63 mmol) was dissolved in THF (20 mL), then AcOH (1 mL) and TBAF (3.32 g, 10.51 mmol) were successively added. The mixture was stirred overnight. The solution was washed with saturated aqueous $NaHCO_3$ (2x15 mL), NaCl (20 mL), the organic phase was dried over $MgSO_4$ and the solvent evaporated. Purification by flash chromatography (Tol) afforded compound **(9)** (0.333 g, 72%) as an clear oil. R_f : 0.17 (Tol:EA; 5:1).

^{1}H NMR (500 MHz, $CDCl_3$) δ_H: 1.33 (4 H, m,-C$\underline{H_2}$C$\underline{H_2}$CH$_2$CH$_2$SAc), 1.51 (4 H, m, -OCH$_2$C$\underline{H_2}$-, -C$\underline{H_2}$CH$_2$SAc), 2.26 (3 H, s, -SCOC$\underline{H_3}$), 2.81 (2 H, t, J = 7.3 Hz, -SC$\underline{H_2}$-), 3.56 (2 H, t, J = 6.6 Hz, -OC$\underline{H_2}$-);
^{13}C NMR (150.9 MHz, $CDCl_3$) δ_C: 25.26, 28.53, 29.03, 29.47 (-C$\underline{H_2}$C$\underline{H_2}$C$\underline{H_2}$C$\underline{H_2}$SAc), 30.62 (-SCOC$\underline{H_3}$), 32.53 (-OCH$_2$C$\underline{H_2}$-), 62.63 (-OC$\underline{H_2}$-), 196.18 (-SCOCH$_3$).
HR-ESI-MS (m/z) calculated for : $C_8H_{16}O_2S$ $(M+Na)^+$ 199.0763, found 199.0768.

6-Trifluoromethanesulfonyloxy-*S*-acetyl-hexan-1-thiol (10)

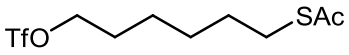

Compound **(9)** (77 mg, 0.437 mmol) was placed under an N_2 (g) atmosphere and suspended in dry DCM (1mL). Lutidine (94 µL, 0.874 mmol) was then added and the solution was cooled to -60°C. Triflic anhydride (96 µL, 0.568 mmol) was added to dry DCM (1mL), cooled to -60°C for a few minutes and then added dropwise to the stirring solution of **(9)**. The reaction was stirred at this temperature for 45 minutes by which time the reaction was complete. The DCM solution was then poured into a separating funnel containing cold saturated KH_2PO_4 (aq.) and washed. The organic layer was separated, dried over $MgSO_4$ and the solvent evaporated (no heating). The crude material was the passed over a short silica plug (DCM). The solvent was evaporated *in vacuo* giving triflate **(10)** as a yellowish oil (135 mg, 67 %). Rf: 0.64 (cyclohexane:DE; 1:1).
^{1}H NMR (500 MHz, $CDCl_3$) δ_H: 1.37 – 1.49 (4 H, m, -OCH$_2$CH$_2$C$\underline{H_2}$C$\underline{H_2}$CH$_2$CH$_2$S-), 1.59 (2 H, m, -C$\underline{H_2}$CH$_2$S-), 1.83 (2 H, m, -OCH$_2$C$\underline{H_2}$-), 2.32 (3 H, s, -SCOC$\underline{H_3}$), 2.86 (2 H, t, J = 7.0, 7.6 Hz), 4.52 (2 H, t, J = 6.4, 6.5 Hz).

(6-Acetylthio-hexy-1-yl) methyl (methylphosphonate) (11)

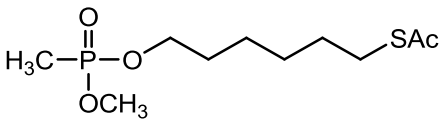

Compound **(9)** (112 mg, 0.635 mmol) was placed under an N_2 (g) atmosphere. Dry DCM (5 mL) was added followed by dry DIPEA (221 µL, 1.27 mmol). The resulting solution was cooled to -15°C (ice/salt-bath) and P(O)(OCH$_3$)(CH$_3$)Cl (82 µL, 0.825 mmol) was added

dropwise. The reaction was allowed to warm to room temperature over the course of 3 hours after which time TLC analysis confirmed the completion of the reaction. MeOH (2 mL) was then added and the solution was stirred for a further 10 minutes. The solvent was removed under vacuum and the crude product was purified directly by flash chromatography (EA) to give compound **(11)** as an oil (135 mg, 79%). Rf: 0.31 (EA).

^{1}H NMR (500 MHz, $CDCl_3$) δ_H: 1.37 (4 H, m, -C$\underline{H_2}$C$\underline{H_2}$CH$_2$CH$_2$SAc), 1.44 (3 H, d, J = 17.5 Hz, P-C$\underline{H_3}$), 1.55 (2 H, m, -SCH$_2$C$\underline{H_2}$-), 1.64 (2 H, m, -OCH$_2$C$\underline{H_2}$-), 2.29 (3 H, s, -SCOC$\underline{H_3}$), 2.83 (3 H, t, J = 7.3 Hz, -SC$\underline{H_2}$-), 3.69 (3 H, d, J = 11.0 Hz, P-OC$\underline{H_3}$), 3.98 (2 H, m, -OC$\underline{H_2}$-);

^{13}C NMR (125.7 MHz, $CDCl_3$) δ_C: ~10.53 (d, J = 144 Hz, P-$\underline{C}$H$_3$), 25.15, 28.36 (-$\underline{C}$H$_2\underline{C}$H$_2$CH$_2$CH$_2$SAc), 29.04 (-$\underline{C}$H$_2$S-), 29.49 (-$\underline{C}$H$_2$CH$_2$S-), ~30.43 (d, J = 6.2 Hz, -OCH$_2\underline{C}$H$_2$-), 30.70 (-SCO$\underline{C}$H$_3$), ~52.15 (d, J = 6.4 Hz, P-O$\underline{C}$H$_3$), ~65.58 (d, J = 6.4 Hz, -O$\underline{C}$H$_2$-), 195.92 (-S$\underline{C}$OCH$_3$);

^{31}P NMR (161.7 MHz, $CDCl_3$) δ_P: 31.81

HR-ESI-MS (m/z) calculated for $C_{10}H_{21}O_4PS$ $(M+Na)^+$ 291.0790, found 291.0787.

6',6'-Dithiobis (hex-1'-yl methyl methylphosphonate) (12)

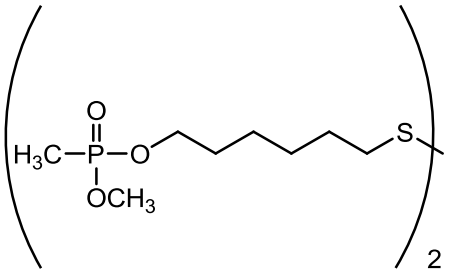

Compound **(11)** (41 mg, 0.155 mmol) was placed under an O_2 (g) atmosphere and was dissolved in anhydrous MeOH (1.5mL). A methanolic NaOMe solution (1.55 mL, 0.1M) was then added dropwise to the stirring solution of **(11)**, ensuring that the O_2 (g) was bubbling through the solution and that indicator paper indicated a pH ~ 10. After stirring overnight, the solvent was evaporated *in vacuo* and the residue was directly purified by flash chromatography (EA:MeOH; 10:1) to give compound **(12)** as an oil (32 mg, 80%). %). R_f: 0.13 (EA:MeOH; 10:1).

^{1}H NMR (500 MHz, $CDCl_3$) δ_H: 1.38 – 1.46 (8 H, m, -C$\underline{H_2}$C$\underline{H_2}$CH$_2$CH$_2$S-), 1.47 (6 H, d, J = 17.5 Hz, P-C$\underline{H_3}$), 1.69 (8 H, m, -OCH$_2$C$\underline{H_2}$CH$_2$CH$_2$C$\underline{H_2}$CH$_2$S-), 2.67 (4 H, t, J = 7.4 Hz, -SC$\underline{H_2}$-), 3.72 (6 H, d, J = 11.1 Hz, P-OC$\underline{H_3}$), 4.02 (4 H, m, -OC$\underline{H_2}$-);

^{13}C NMR (125.7 MHz, $CDCl_3$) δ_C: ~10.59 (d, J = 144 Hz, P-CH_3), 25.34, 28.16 (-OCH_2CH_2-$\underline{C}H_2\underline{C}H_2$-$CH_2CH_2S$-), 29.18 (-$\underline{C}H_2CH_2S$-), ~30.54 (d, J = 6.2 Hz, -$OCH_2\underline{C}H_2$-), 39.03 (-$\underline{C}H_2S$-), ~52.22 (d, J = 6.3 Hz, P-$O\underline{C}H_3$), ~65.67 (d, J = 6.5 Hz, -$O\underline{C}H_2$-);

^{31}P NMR (161.7 MHz, $CDCl_3$) δ_P: 31.87 (s).

HR-ESI-MS (m/z) calculated for $C_{16}H_{36}O_6P_2S_2$ $(M+Na)^+$ 473.1321, found 473.1325.

6',6'-Dithiobis (ammonium [hex-1'-yl methyl methylphosphonate]) (13)

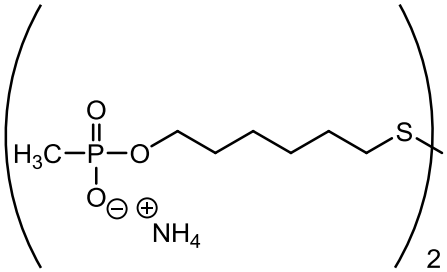

Compound **(12)** (80 mg, 0.178 mmol) and sodium iodide (269 mg, 1.78 mmol) were dried under vacuum in the absence of light for 20 minutes and then placed under an N_2 (g) atmosphere. Dry acetone (2 mL) was then added to the reaction flask followed by ultrasonication. The solution was then refluxed over 48 hours by which time TLC had indicated the absence of starting material and the formation of a new baseline spot. The solvent was removed under vacuum and purified by flash chromatography (EA:MeOH; 5:1 → MeOH) to give compound **(13)** as a white solid after subsequent gel filtration and lyophilisation (60 mg, 80%). R_f: 0.26 (EA/MeOH; 1:1).

^{1}H NMR (500 MHz, MeOH-D_4) δ_H: 1.22 (6 H, d, J = 16.4 Hz, P-$C\underline{H}_3$), 1.43 (8 H, m, -$C\underline{H}_2C\underline{H}_2CH_2CH_2S$-), 1.62 (4 H, tt, J = 6.4, 7.0 Hz, -$OCH_2C\underline{H}_2$-), 1.69 (4 H, p, J = 7.0 Hz, -$C\underline{H}_2CH_2S$-), 2.69 (4 H, t, J = 7.1, 7.3 Hz, -$C\underline{H}_2S$-), 3.83 (4 H, dt, J = 6.5, 6.5 Hz, -$OC\underline{H}_2$-);

^{13}C NMR (100.5 MHz, MeOH-D_4) δ_C: ~12.43 (d, J = 137 Hz, P-$\underline{C}H_3$), 26.59, 29.22 (-$\underline{C}H_2\underline{C}H_2CH_2CH_2S$-), 30.20 (-$\underline{C}H_2CH_2S$-), ~31.98 (d, J = 6.8 Hz, -$OCH_2\underline{C}H_2$-), 39.63 (-$\underline{C}H_2S$-), ~64.88 (d, J = 5.6 Hz, -$O\underline{C}H_2$-);

^{31}P NMR (161.7 MHz, MeOH-D_4) δ_P: 24.19 (s).

HR-ESI-MS (m/z) calculated for $C_{14}H_{32}O_6P_2S_2$ $(M+3Na)^+$ 489.0647, found 489.0645.

Nanoparticle Syntheses

'Small' phospha-oseltamivir stabilised gold nanoparticles ("small TamiGold")

Disulfide **(4)** (3.5 mg, 4.02 x 10^{-3} mmol) was dissolved in MeOH (0.4 mL). The methanolic solution was added to an aqueous solution of 0.025M $HAuCl_4.3H_2O$ (1.34 x 10^{-3} mmol) followed by acetic acid (5.4 µL, 0.0938 mmol). Vigorous stirring over 15 minutes was followed by subsequent addition of freshly prepared aqueous 1M sodium borohydride (0.0268 mmol) in two portions over 5 minutes. The resulting brown/black solution was stirred overnight in the absence of light. The solvent was removed *in vacuo* to near dryness where the resulting waxy product was co-evaporated with MilliQ water (x2). MilliQ water (low volume) was added to the residue to aid the solubility of the nanoparticles for transfer to an eppendorf tube. Cycles of centrifugation (~12000g) and resuspension with ethyl acetate/methanol (10:1 → 5:1) were repeated until the supernatant showed no starting material (by TLC). The black/brown particulate suspension was resuspended in MilliQ water and dialysed against MilliQ water over 7 days (7 x 1 L).

'Small' monomethylphosphonate-stabilised gold nanopaticles (control)

A procedure identical to that of phospha-oseltamivir-stabilised gold nanopaticles described above was used, with disulfide **(13)** as ligand. The black/brown residue formed in the reaction showed a lower solubility in MeOH as compared to "small TamiGold". Ethyl acetate/methanol ratios used in the centrifugation process were adjusted accordingly.

'Large' phospha-oseltamivir-stabilised gold nanoparticles ('large TamiGold')

Freshly prepared citrate-capped gold nanoparticles (for synthesis, see below) (~3 nM, 10 mL) were added to a solution of disulfide **(4)** (6 mg, 0.00689 mmol) in 10mM phosphate buffer (pH ~7.6) (1 mL). After 30 minutes, UV spectroscopy confirmed a slight red-shift of the gold nanoparticle suspension (519 nm to 525 nm). The solution was stirred vigorously for a further 72 hours in the absence of light to ensure the place exchange reaction reached completion. The volume of the AuNP solution was then reduced *in vacuo* (no heating) to ~ 4 mL. The red coloured solution was then transferred to a 50 mL centrifuge tube and acidified to pH 2-3 (indicator paper) with 0.1 M HCl (aq.) in order to induce nanoparticle aggregation (red to

purple colour change). The solution was then centrifuged after which the supernatant was removed carefully. Deionised H_2O (acidified to ~ pH 3) was added to the purple aggregate which was then agitated, followed by further centrifugation. This process was repeated until disulfide **(4)** was no longer detected (TLC and ^{1}H NMR of supernatant residue). A few drops of 0.1 M NaOH (aq.) were added to the purple aggregate (which turned red) followed by 1 mL of Tris buffer (10 mM, pH 9.3) (2 mL). If necessary another drop of 0.1 M NaOH (aq.) was added to ensure all aggregated particles were resuspended (solution ~ pH 9.5 – 10, indicator paper). The resulting red solution was diluted with Tris buffer (final volume 5 mL) and underwent prolonged dialysis with Tris buffer (10 mM, pH 9.3) (2 L x 7 days). A final solution pH of ~9.3 was confirmed with the use of a pH meter.

Synthesis of citrate-capped gold nanoparticles[11]

An 100 mL aqueous solution of $HAuCl_4.3H_2O$ (13.8 mg, 0.0350 mmol) was continuously stirred and heated to 60°C. A 50 mL aqueous trisodium citrate solution (55.5 mg, 0.215 mmol) was heated to 60°C and then rapidly added to the stirring chloroauric acid solution. Heating and vigorous stirring was maintained for ~ 2 hours until a wine red solution was obtained with characteristic UV band (~ 519 nm).

Nanoparticle Analyses

Transmission electron microscopy (TEM and HR-TEM)

Transmission electron microscopy (TEM) and high resolution transmission electron microscopy (HR-TEM) were carried out using a Hitachi-7100 Transmission Electron Microscope (accelerating voltage of 100kV) and a JEOL 4000EX HREM (accelerating voltage of 400kV) respectively. Samples were prepared by dropping aqueous nanoparticle suspensions on Formvar-coated holey copper grids (TEM) or lacey carbon grids (HRTEM) and allowing the samples to air-dry. Samples for HRTEM were baked on a 60 W lamp before imaging. Staining was carried out using uranyl acetate (2%). Electron micrograph images were analysed using ImageJ (Rasband, W.S., ImageJ, U. S. NIH, Bethesda, Maryland, USA, http://rsb.info.nih.gov/ij/, 1997-2011). Images underwent limited editing to improve contrast for counting purposes where necessary. Particles were counted with the automated particle analysis tool or manually where necessary (by measuring the longest vertical particle diameter). All image analysis was carried out by the same operator using ~ 200 particles for statistical analysis.

Diffusion Ordered Spectroscopy (DOSY) NMR

Stokes-Einstein equation for the calculation of the hydrodynamic radius of a spherical particle from its diffusion coefficient:

$D = kT / 6 \pi \eta r_H$

D = diffusion coefficient from DOSY experiment

η (viscosity) = 8.9×10^{-4} Pa s (for H_2O at 298 K)

k = Boltzmann's constant

r_H ~ hydrodynamic radius

M. Nilsson, et al., The DOSY Toolbox: A new tool for processing PFG NMR diffusion data. *Journal of Magnetic Resonance* **2009**, 200, 296-302.

Energy dispersive x-ray analysis (EDX)

Energy dispersive x-ray analysis (EDX) was performed using an Oxford INCA Energy 200 Premium instrument connected to a JEOL JSM 5900LV scanning electron microscope. The solid sample was deposited onto an aluminium pin stub using double-sided adhesive carbon discs (Agar Scientific Ltd). The sample was viewed using 3 kV primary beam accelerating voltage and an in-lens distance of 5 mm. Data recording from the selected positions was performed over a period of 50 seconds.

Dynamic light scattering (DLS)

Size measurements were performed using dynamic light scattering (DLS) on a Malvern Zetasizer Nano-S (Malvern Instruments, Malvern, UK). Samples were irradiated with red light (HeNe laser, wavelength $\lambda = 632.8$ nm) and the intensity fluctuations of the scattered light (detected at a backscattering angle of 173°) was analysed (avalanche photodiode (APD) detector) to obtain an autocorrelation function. The software (DTS v5.00) provided both the size mean and polydispersity, using the cumulants analysis and a size distribution using a regularization scheme by intensity (and by volume and number where applicable). Samples were filtered before analysis, once over a cotton plug followed by a disposable 0.45µm filter to remove any unwanted contaminants and large aggregates.
The following assumptions were made in the analysis: the solution viscosity was assumed to be that of water, corrected for temperature ($\eta = 0.8872$ mPa.s); the solution refractive index was that of water ($n = 1.33$); the refractive index of the particle was selected to be $nR = 0.34$ with absorption of $nI = 2.37$.[10] Samples were measured in disposable Eppendorf UVette 50-2000 µL polystyrene cuvettes at a temperature of 25°C, and this temperature was actively maintained within 0.1°C . Data were acquired in automatic mode (3 measurements x 12 runs), ensuring enough photons were accumulated for the result to be statistically relevant. The software incorporated a ‘data quality report’ that indicated good quality for all data obtained.

UV-Visible spectroscopy

UV-Visible spectra were recorded on a Varian Cary 50 Scan spectrometer using the fast scan setting. Spectra of nanoparticle suspensions were recorded with deionised water, Tris buffer (10 mM, pH 9.3) or phosphate buffer (10 mM, pH 7.6) as a blank reference in a 1 mL cuvette (1 cm path length).

Calculation of concentration of 'small TamiGold' and phospha-oseltamivir moieties in inhibition assays

Ratio (Au/phospha-oseltamivir) = 1:1 based on EDX-analysis of the Au/S ratio.

Number of Au atoms/particle for a diameter of 2 nm: ~ 200.[12]
$n_{Au} = 4\Pi(d/2)^3/3Vg$ with d = diameter of particle; Vg = volume of gold atom (fcc) = 17 $Å^3$

This results in an estimate of 200 Au atoms and 200 phospha-oseltamivir moieties per particle, thus giving a molecular weight per particle of $m_{Particle}$ = 126500 Da (200 x m_{Au} + 200 x ($m_{Compound\ 4}$)/2).

Concentrations of 'small TamiGold' and phospha-oseltamivir moieties in stock solution used for inhibition assays:

Particle concentration: 1 mg/mL (particle) = 7.9 x 10^{-6} mM/mL (particle).
Phospha-oseltamivir concentration for 1 mg/mL (particle) = 1.6 x 10^{-3} mM/mL = 1.6 mM.

The same assumptions and calculations were used for the methylphosphonate-stabilised control particles, resulting in a 2.3 mM stock solution.

Inhibition of neuraminidase activity by dimeric ligand 4

A whole virus assay using allantoic fluid from infected eggs was used. In brief, neuraminidase (NA) enzymatic activity was studied using the fluorescent substrate 2'-4-methylumbelliferyl)-α-D-*N*-acetylneuraminic acid (MUNANA). Measurements were made at 37 °C in 32.5 mM MES (pH 6.5) + 4 mM $CaCl_2$ using a JASCO FP-6300 fluorimeter with excitation at 365 nm and emission at 450 nm. Michaelis-Menten constants for the enzyme, $K_m = (k_2 + k_{-1})/k_1$, were determined using standard initial rate measurements with estimated neuraminidase concentrations in the range 0.1 to 0.5 nM and MUNANA concentrations in the range 2 to 200 μM.

Inhibition constants (K_I) were determined by measuring the extent to which different concentrations of inhibitor reduced the steady-state rate of MUNANA hydrolysis. The data were interpreted using the following simple model for competitive inhibition in which E, S, and I represent neuraminidase, MUNANA, and inhibitor, respectively:

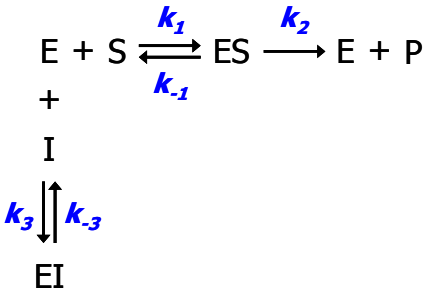

The reduced rate of hydrolysis of MUNANA observed in the presence of inhibitor is predicted by the following equation (Rameix-Welti et *al.*)[13]:

$$V_I = \frac{V_0([S] + K_m)}{[S] + K_m\left(1 + \frac{[I]}{K_I}\right)} \qquad (1)$$

where V_I is the steady-state rate for MUNANA hydrolysis in the presence of inhibitor at concentration [I], V_0 is the steady-state rate for MUNANA hydrolysis in the absence of inhibitor, [S] is the MUNANA concentration, K_m is the Michaelis-Menten constant for hydrolysis of MUNANA, and K_i is the dissociation constant for the enzyme-inhibitor complex. Because these inhibitors show a slow approach to the new steady state rate (see Collins et *al.*[S6]) it was necessary to confirm that the new steady-state rate had been reached;

this was done by demonstrating that the first derivative of the fluorescence change (proportional to the NA activity) became constant at long times.

Inhibition of seasonal and pandemic influenza virus strains assays by "small TamiGold" and methylphosphonate-stabilised gold nanoparticles (control)

Neuraminidase inhibition assays with "small TamiGold" and methylphosphonate-stabilised control gold nanoparticles were carried out according to standard procedures at the Division of Virology and WHO Collaborating Centre for Influenza Reference and Research, Mill Hill, London, UK.

Virus samples: Virus from tissue culture fluid

Protocol: SOP No 25/C2
FLUORESCENT (MUNANA) NEURAMINIDASE INHIBITION ASSAY FOR INFLUENZA VIRUS DRUG SUSCEPTIBILITY DETERMINATION

The inhibition of virus sialidase activity was carried out on the low molecular weight substrate 2'-(4-methylumbelliferyl)-α-D-*N*-acetyl neuraminic acid (MUNANA). The assay, carried out in black 96 well flat bottom plates (Corning, 3915), in 6.05 mmol/l MES, 0.8 mmol/l $CaCl_2$, pH6.5 and 60 micromol/l MUNANA in a 50 microlitre assay was carried out for 60 min at 37^o; the reaction was terminated by the addition of 3 volumes of stop buffer 0.1 mole/l glycine pH 10.7 in 25% ethanol. Virus was initially titrated to estimate a dilution that results in the production of 10 micromol/l of 4-methylumbelliferone in the assay. Fluorescence was measured on a Tecan, Safire2 microplate reader. (with excitation at 355 nM and emission at 460 nM).

References (supporting information):

1. The monosilylated precursor of compound **7** was prepared according to standard literature procedures; *Protective Groups in Organic Synthesis*, Third Edition, T. W. Greene, P. G. M. Wuts, **1999**, John Wiley & Sons, Inc., 119-148.

2. Y. Xu, S. A. Lee, T. G. Kutateladze, D. Sbrissa, A. Shisheva, G. D. Prestwich, *J. Am. Chem. Soc.*, **2006**, 128(3), 885-897.

3. C. López-Cartes, T. C. Rojas, R. Litrán, D. Martínez-Martínez, J. M. de la Fuente, S. Penadés, A. Fernández, *The Journal of Physical Chemistry B*, **2005**, 109, 8761-8766.

4. *Encyclopedia of Materials Characterisation, Surfaces, Interfaces, Thin Films*, Eds., R. C. Brundle, C. A. Evans, S. Wilson, **1992**, Elsevier; Chapter 3.1, *Energy Dispersive X-ray Spectroscopy*, EDS, R. Geiss, 120-121.

5. L. V. Gubareva, L. Kaiser, M. N. Matrosovich, Y. Soo-Hoo, *J Infect Dis. (2001) 183(4): 523-531*

6. S. L. Westcott, S. J. Oldenburg, T. R. Lee, N. J. Halas, Chem. Phys. Lett., **1999**, 300, 651 – 655.

7. R. Elghanian, J. J. Storhoff, R. C. Mucic, R. L., Letsinger, C. A. Mirkin, Science, **1997**, 1078 – 1081.

8. D. C. Hone, A. H. Haines, D. A. Russell, Langmuir, **2003**, 19, 7141 – 7144.

9. B. Carbain, P. J. Collins, L. Callum, S. R. Martin, A. J. Hay, J. McCauley, and H. Streicher, *ChemMedChem*, 2009, **4**, 335-337.

10. L. G. Schulz, F. R., Tangherlini, *J. Opt. Soc. Am.*, **1954**, 44 (5), 357 – 368.

11. C. L. Schofield, A. H. Haines, R. A. Field, D. A. Russell *Langmuir* **22**, 6707 – 6711 (2006).

12. M.-C. Daniel, D. Astruc, Chem. Rev. 2004, 104, 293-346.

13. M. A. Rameix-Welti, , F. Agou, P. Buchy, S. Mardy, J. T. Aubin, M. Veron, S. van der Werf, N. Naffakh, *Antimicrobial Agents Chemother*. **2006**, *50*, 3809-3815.